Article:

Asseng, S, Martre, P, Maiorano, A et al. (64 more authors) (2019) Climate change impact and adaptation for wheat protein. Global Change Biology, 25 (1). pp. 155-173. ISSN 1354-1013

https://doi.org/10.1111/gcb.14481

24 Sept 2018

Supplementary Materials for

Climate change impact and adaptation for wheat protein

S. Asseng, P. Martre, A. Maiorano, R.P. Rötter, G.J. O'Leary, G.J. Fitzgerald, C. Girousse, R. Motzo, F. Giunta, M.A. Babar, M.P. Reynolds, A.M.S. Kheir, P.J. Thorburn, K. Waha, A.C. Ruane, P.K. Aggarwal, M. Ahmed, J. Balkovic, B. Basso, C. Biernath, M. Bindi, D. Cammarano, A.J. Challinor, G. De Sanctis, B. Dumont, E. Eyshi Rezaei, E. Fereres, R. Ferrise, M. Garcia-Vila, S. Gayler, Y. Gao, H. Horan, G. Hoogenboom, R.C. Izaurralde, M. Jabloun, C.D. Jones, B.T. Kassie, K.C. Kersebaum, C. Klein, A.-K. Koehler, B. Liu, S. Minoli, M. Montesino San Martin, C. Müller, S. Naresh Kumar, C. Nendel, J.E. Olesen, T. Palosuo, J.R. Porter, E. Priesack, D. Ripoche, M.A. Semenov, C. Stöckle, P. Stratonovitch, T. Streck, I. Supit, F. Tao, M. Van der Velde, D. Wallach, E. Wang, H. Webber, J. Wolf, L. Xiao, Z. Zhang, Z. Zhao, Y. Zhu, and F. Ewert

Supplementary Materials and Methods

Table S1. List of the 32 wheat crop models used in the AgMIP Wheat study.

Code	Name (version)	Reference	Documentation
AE	APSIM-E*	(Chen *et al.*, 2010a, Keating *et al.*, 2003, Wang *et al.*, 2002)	http://www.apsim.info/Wiki
AF	AFRCWHEAT2*	(Porter, 1984, Porter, 1993, Weir *et al.*, 1984)	Request from John Porter: jrp@plen.ku.dk
AQ	AQUACROP (V.4.0)	(Steduto *et al.*, 2009)	http://www.fao.org/nr/water/aquacrop.html
AW	APSIM-Wheat (V.7.3)*	(Keating *et al.*, 2003)	http://www.apsim.info/Wiki
CS	CropSyst (V.3.04.08)	(Stockle *et al.*, 2003)	http://modeling.bsyse.wsu.edu/CS_Suite_4/CropSyst/index.html
DC	DSSAT-CERES-Wheat (V.4.0.1.0)*	(Hoogenboom & White, 2003, Jones *et al.*, 2003, Ritchie *et al.*, 1985)	http://dssat.net/
DN	DSSAT-Nwheat*	(Asseng, 2004, Kassie *et al.*, 2016)	http://dssat.net/
DR	DSSAT-CROPSIM (V4.5.1.013)*	(Hunt & Pararajasingham, 1995, Jones *et al.*, 2003)	http://dssat.net/
DS	DAISY (V.5.24)*	(Hansen *et al.*, 2012, Hansen *et al.*, 1991)	http://daisy.ku.dk
EI	EPIC-I (V0810)	(Balkovič *et al.*, 2013, Balkovič *et al.*, 2014, Kiniry *et al.*, 1995, Williams, 1995, Williams *et al.*, 1989)	http://epicapex.tamu.edu/epic
EW	EPIC-Wheat(V1102)	(Izaurralde *et al.*, 2006, Izaurralde *et al.*, 2012, Kiniry *et al.*, 1995,	http://epicapex.brc.tamus.edu

		Williams, 1995, Williams *et al.*, 1989)	
GL	GLAM (V.2 updated)	(Challinor *et al.*, 2004, Li *et al.*, 2010)	https://www.see.leeds.ac.uk/research/icas/research-themes/climate-change-and-impacts/climate-impacts/glam
HE	HERMES (V.4.26)*	(Kersebaum, 2007, Kersebaum, 2011)	http://www.zalf.de/en/forschung/institute/lsa/forschung/oekomod/hermes
IC	INFOCROP (V.1)	(Aggarwal *et al.*, 2006)	http://infocrop.iari.res.in/wheatmodel/UserInterface/HomeModule/Default.aspx
LI	LINTUL4 (V.1)	(Shibu *et al.*, 2010, Spitters & Schapendonk, 1990)	http://models.pps.wur.nl/node/950
L5	SIMPLACE<Lintul-5* SlimWater3,FAO-56, CanopyT,HeatStressHourly	(Gaiser *et al.*, 2013, Shibu *et al.*, 2010, Spitters & Schapendonk, 1990, Webber *et al.*, 2016)	http://www.simplace.net/Joomla/
LP	LPJmL (V3.2)	(Beringer *et al.*, 2011, Bondeau *et al.*, 2007, Fader *et al.*, 2010, Gerten *et al.*, 2004, Müller *et al.*, 2007, Rost *et al.*, 2008)	http://www.pik-potsdam.de/research/projects/lpjweb
MC	MCWLA-Wheat (V.2.0)	(Tao *et al.*, 2009a, Tao & Zhang, 2010, Tao & Zhang, 2013, Tao *et al.*, 2009b)	Request from taofl@igsnrr.ac.cn
MO	MONICA (V.1.0)*	(Nendel *et al.*, 2011)	http://monica.agrosystem-models.com
NC	Expert-N (V3.0.10) – CERES (V2.0)*	(Biernath *et al.*, 2011, Priesack *et al.*, 2006, Ritchie *et al.*, 1987, Stenger *et al.*, 1999)	http://www.helmholtz-muenchen.de/en/iboe/expertn
NG	Expert-N (V3.0.10) – GECROS (V1.0)*	(Biernath *et al.*, 2011, Stenger *et al.*, 1999)	http://www.helmholtz-muenchen.de/en/iboe/expertn
NP	Expert-N (V3.0.10) – SPASS (2.0)*	(Biernath *et al.*, 2011, Priesack *et al.*, 2006, Stenger *et al.*, 1999,	http://www.helmholtz-muenchen.de/en/iboe/expertn

		Wang & Engel, 2000, Yin & van Laar, 2005)	
NS	Expert-N (V3.0.10) – SUCROS (V2)	(Biernath *et al.*, 2011, Goudriaan & Van Laar, 1994, Priesack *et al.*, 2006, Stenger *et al.*, 1999)	http://www.helmholtz-muenchen.de/en/iboe/expertn
OL	OLEARY (V.8)*	(Latta & O'Leary, 2003, OLeary & Connor, 1996a, OLeary & Connor, 1996b, Oleary *et al.*, 1985)	Request from gjoleary@yahoo.com
S2	Sirius (V2014)*	(Jamieson & Semenov, 2000, Jamieson *et al.*, 1998, Lawless *et al.*, 2005, Semenov & Shewry, 2011)	http://www.rothamsted.ac.uk/mas-models/sirius.php
SA	SALUS (V.1.0)*	(Basso *et al.*, 2010, Senthilkumar *et al.*, 2009)	http://salusmodel.glg.msu.edu
SP	SIMPLACE<Lintul-2 CC,Heat,CanopyT,Re-Translocation	(Angulo *et al.*, 2013)	http://www.simplace.net/Joomla/
SQ	*SiriusQuality* (V3.0)*	(Ferrise *et al.*, 2010, He *et al.*, 2010, Maiorano *et al.*, 2017, Martre *et al.*, 2006)	http://www1.clermont.inra.fr/siriusquality
SS	SSM-Wheat	(Soltani *et al.*, 2013)	Request from afshin.soltani@gmail.com
ST	STICS (V.1.1)*	(Brisson *et al.*, 2003, Brisson *et al.*, 1998)	http://www6.paca.inra.fr/stics_eng
WG	WheatGrow (V3.1)	(Cao *et al.*, 2002, Cao & Moss, 1997, Hu *et al.*, 2004, Li *et al.*, 2002, Pan *et al.*, 2007, Pan *et al.*, 2006, Yan *et al.*, 2001)	Request from yanzhu@njau.edu.cn
WO	WOFOST (V.7.1)	(Boogaard & Kroes, 1998)	http://www.wofost.wur.nl

*Models that have routines to simulate crop and grain nitrogen dynamics leading to grain protein and have been tested with field measurements before. These 18 models have been used in the grain protein analysis.

Field experiments for model testing

INRA temperature experiment

In all INRA experiments, crops were grown outside in 2 m^2 containers with 0.5 m depth, filled with a 2:1 (v:v) mixture of black soil and peat. Seeds were sown on 10 November 1999, 08 November 2000, and 07 November 2006 at 2.5 cm from the soil surface with a density of 578 seeds m^{-2} and a row spacing of 6.25 cm, resulting in 554 to 666 fertile tillers m^{-2} at anthesis, mimicking field density and plant competition. The high plant density inhibited the development of axillary tillers, which coordinated the development of the crops within and between the containers. In 1999 and 2000, ammonium phosphate (N: P, 18:46; 20 g m^{-2}) and potassium sulphate (K_2SO_4; 20 g m^{-2}) were hand-dressed at sowing. The preceding crops were sunflower and wheat, and three years fallow in 1999, 2000, and 2006. During the wheat growth period, crops were fertilized with ammonium-nitrate or ammonium-phosphate and received a total of 15 to 20 g N m^{-2} in two to three applications between one week after the beginning of tillering and male meiosis. From sowing to anthesis the crops received the following amounts of rainfall: 199 mm (1999-2000), 247 mm (2000-2001), and 145 mm (2006-2007). In addition, during that period the crops received the following irrigation amounts to maintain the soil water content above 80% of field capacity: 208 mm (1999-2000), 90 mm (2000-2001), and 143 mm (2006-2007). At anthesis, all the containers were irrigated to field capacity by applying 90 mm of water, they then received 6 to 50 mm of water every 2 to 7 days until maturity to replace measured crop evapotranspiration. Spikes were tagged at anthesis to allow accurate determination of the developmental stage when harvesting. All other crop inputs, including disease and pest control, were applied at levels to prevent diseases and pests from limiting plant growth and grain yield.

Between 1 and 5 d after anthesis the containers were transferred under transparent enclosures under natural light in the Crop Climate Control and Gas Exchange Measurement (C3-GEM) experimental platform. The C3-GEM platform allows monitoring and controlling air temperature, air CO_2 concentration, water supply, and gas exchange of up to four 2 m^2 containers (Triboï *et al.*, 1996). Air CO_2 concentration was maintained at 378 ± 5 ppm. Different temperature regimes were applied under the enclosures. In 2000, day/night air temperatures were controlled at 18 °C/10 °C (control treatment) or at 28 °C/15 °C (chronic high temperature treatment). Heat shocks consisting of two consecutive days with air temperature of 38 °C for 3 h between 11:30 and 14:30 solar time during the first day and 6 h between 10:15 and 16:15 solar time during the second day were applied starting 30 days after anthesis (i.e., during the linear grain filling period) on one container maintained at the cooler temperature regime the rest of the time. In 2001, all containers were maintained at 18 °C/10 °C (day/night) and heat shocks consisting of 4 h a day at 38 °C (air temperature), between 10:00 and 14:00 solar time and 20 °C (air temperature) the rest of the day were applied for four consecutive days starting 7 days after anthesis (i.e., during the endosperm cell division period) or 18 days after anthesis (i.e., during the linear grain filling period). In 2007, all containers were maintained at 21°C/14°C (day/night) and heat shocks consisting of 4 h a day at 38 °C (air temperature), between 10:00 and 14:00 solar time and 21 °C (air temperature) the rest of the day were applied for four consecutive days during either the endosperm cell division period (starting 8 days after anthesis), the linear grain filling period (starting 23 days after anthesis), or during both phases. The rate of heating or cooling before and after the heat shocks was 8.5°C h^{-1}. Air relative humidity was maintained between 65% and 80%, corresponding to a vapor pressure deficit (VPD) of 0.5/0.3 kPa (day/night) in 2000 and 2001, and 0.6/0.4 kPa (day/night) in 2007. During the 4 h of heat shock, the air relative humidity ranged from 40% to 50% and the air VPD from 3.0 to 3.7 kPa.

To study the dynamic accumulation of dry mass and total N in leaves, stems, chaffs, and grains, three replicates of 20 plants were collected in each container every 2 to 9 days from anthesis to grain maturity. At maturity 0.4 to 1.25 m^2 were harvested. Samples were collected starting from the south. Stems, leaves, chaffs, and grains were separated, and their dry mass was determined after oven drying at 80 °C to a constant mass. Total N content of oven-dried samples was determined by the Kjeldhal method using a Kjeltec 2300 analyser (Foss Tecator AB, Hoeganaes, Sweden) in 2000 and 2001, and by the Dumas combustion method using a FlashEA 1112 N/Protein analyser (Thermo Electron Corp., Waltham, MA, USA) in 2007. Grain protein concentration was calculated from the percentage of total N by multiplying by a conversion factor of 5.62 for grains of wheat (Mossé *et al.*, 1985).

Table S2. Layout of the experiment treatments of the INRA Clermont-Ferrand temperature experiments. Grain yield and protein data are medians and the 25th and 75th quantiles between squared brackets.

Treatment name	**Sowing date**	**Post-anthesis day/night air temperature (°C)**	**Treatment description**	**Grain yield (t DM ha^{-1})**	**Grain protein (% of yield)**
HSE01_CTRL	10-Nov-99	18/10	Control	7.94 [7.87-8.02]	10.28 [10.28-10.29]
HSE02_HS1	10-Nov-99	18/10	Heat shock during the grain filling lag period (2 days at T_{max} 38°C during 4 hours)	7.98 [7.87-8.07]	12.23 [12.06-12.17]
HSE03_HT	10-Nov-99	28/15	Chronic high temperature during grain filling	6.22 [6.05-6.38]	12.29 [12.25-12.45]
HSE04_CTRL	08-Nov-00	18/10	Control	8.45 [8.45-8.45]	10.28 [10.27-10.34]
HSE05_HS1	08-Nov-00	18/10	Heat shock during the grain filling lag period (4 days at T_{max} 38°C during 4 hours)	6.67 [6.67-6.67]	12.13 [12.13-12.28]
HSE06_HS2	08-Nov-00	18/10	Heat shock during the linear grain filling period (4 days at T_{max} 38°C during 4 hours)	7.45 [7.45-7.45]	12.59 [12.52-12.77]
HSE07_CTRL	07-Nov-06	21/14	Control	6.93 [6.75-7.32]	11.52 [11.27-11.66]
HSE08_HS1	07-Nov-06	21/14	Heat shock during the grain filling lag period (4 days at T_{max} 38°C during 4h)	7.01 [6.28-7.32]	11.66 [11.52-12.13]
HSE09_HS12	07-Nov-06	21/14	Heat shock during both the grain filling lag period and the linear grain filling	5.6 [5.37-5.83]	13.46 [13.57-13.32]

			period (2 x 4 days at T_{max} 38°C during 4h)		
HSE10_HS2	07-Nov-06	21/14	Heat shock during the linear grain filling period (4 days at T_{max} 38°C during 4h)	6.31 [5.44-6.63]	12.69 [13.14-12.73]

AGFACE Australia experiment (CO_2 × temperature × water)

The agronomic design of the AGFACE Australia experiment with the two times of sowing over three years (2007-2009) comprised a complete randomized block experimental design of four replicates. Sowing time altered biomass partitioning including yield because crops are forced to develop into warmer, less efficient conditions as summer approaches.

Gravimetric soil water content was measured at sowing and harvest using a hydraulically operated soil sampler. Sampling was done for layers 0-0.1m and 0.1-0.2m and for 0.2 m increments thereafter to 2 m from one core per plot (42 mm diameter cores). Soil mineral nitrogen (NO_3 and NH_4) was also measured from an additional core taken close to the sampling time of the soil water measurements. Soil bulk density was measured from 70 mm diameter × 75 mm deep sampling rings from each octagonal area. Large soil mineral nitrogen content (~300 kg N ha^{-1}) at the site precluded any significant effects of applied N, so soil analyses were pooled across the N treatments.

Biomass samples taken at stem elongation (DC31), anthesis (DC65), and maturity (DC90) were oven dried at 70ºC and leaf and stem area measurements were made from using an electronic planimeter from subsamples comprising approximately 25% of the collected fresh biomass. Mean sowing plant density measured by plant counts approximately three weeks after emergence was 120 plants m^{-2} and ranged from 60 to 175 plants m^{-2}. Grain yield was measured at maturity including its component grain number per m^2 and grain dry mass and nitrogen content. Agronomic management at both sites was according to local practices, including spraying fungicides and herbicides, as needed. Granular phosphorus and Sulphur (i.e., 'superphosphate') were incorporated into the soil at sowing at rates between 7 and 9 kg P ha^{-1} and 8 and 11 kg S ha^{-1} depending on the year. Because of large variability across the experimental site, the initial soil water content at sowing across the ambient and elevated CO_2 treatments were pooled to be consistent with single soil type parameters for the site (O'Leary *et al.*, 2015).

Table S3. Summary of 18 selected treatments used to compare the simulated and observed grain yield and grain protein concentration from the Horsham FACE experiment (AGFACE). Grain yield and protein data are medians and the 25th and 75th quantiles between squared brackets.

Treatment name	**Sowing date**	**CO_2 (ppm)**	**Sowing**	**Irrigation (mm)**	**Applied N (kg N ha^{-1})**	**Grain yield (t DM ha^{-1})**	**Grain protein (% of yield)**
A7T1 + N+I	18-Jun-07	365	Early	96	138	3.15 [3.06-3.23]	15.28 [15.45-15.17]
E7T1+N+I	18-Jun-07	550	Early	96	138	4.17 [3.73-4.66]	14.76 [14.79-14.67]
A7T2 +N+I	23-Aug-07	365	Late	96	138	2.04 [1.34-2.81]	15.37 [15.79-15.07]
E7T2+N+I	23-Aug-07	550	Late	96	138	3.25 [2.92-3.8]	14.65 [15.11-14.4]
A7T2+N-I	23-Aug-07	365	Late	48	138	2.09 [1.81-2.39]	15.49 [15.67-15.29]
E7T2+N-I	23-Aug-07	550	Late	48	138	2.15 [1.86-2.4]	15.47 [15.7-15.2]
A8T1+N+I	04-Jun-08	365	Early	40	53	2.86 [2.41-3.48]	18.47 [19.35-17.75]
E8T1+N+I	04-Jun-08	550	Early	40	53	3.88 [3.5-4.46]	17.06 [17.75-15.79]
A8T2+N+I	05-Aug-08	365	Late	80	53	1.83 [1.7-1.92]	17.74 [18.41-17.28]
E8T2+N+I	05-Aug-08	550	Late	80	53	2.09 [1.67-2.48]	16.17 [16.6-16.2]
A8T2+N-I	05-Aug-08	365	Late	25	53	1.43 [1.33-1.48]	16.81 [16.77-16.91]
E8T2+N-I	05-Aug-08	550	Late	25	53	0.89 [0.68-1.24]	18.39 [18.99-17.71]
23-Jun-09	23-Jun-09	365	Early	70	53	2.56 [2.18-2.89]	17.16 [17.57-17.13]

23-Jun-09	23-Jun-09	550	Early	70	53	3.04 [2.72-3.3]	15.03 [14.91-15.94]
19-Aug-09	19-Aug-09	365	Late	60	53	1.24 [1.14-1.38]	18.93 [19.22-18.72]
19-Aug-09	19-Aug-09	550	Late	60	53	1.79 [1.32-2.34]	18.86 [18.71-18.25]
19-Aug-09	19-Aug-09	365	Late	0	53	0.98 [0.84-1.17]	21.51 [21.9-19.9]
19-Aug-09	19-Aug-09	550	Late	0	53	1.61 [1.43-1.93]	18.72 [18.96-17.41]

Field experiments for adaptation

Egypt experiment

Experimental data from Egypt were collected from four field experimental sites along the river Nile over three growing seasons (2011/2012, 2012/2013 and 2013/2014).These locations were based on the variability of agro-climatic zones in Egypt from North to South (Khalil *et al.*, 2011). The locations from North (moderate temperature) to South (high temperature) were as follows: Sakha (North delta, lower Egypt, 31.0° N, 30.9° E, 5 m elevation); Menofya (Middle delta, 30.7° N, 31.0° E, 10 m elevation); Benisuef (Middle Egypt, 29.1° N, 31.0° E, 30 m elevation); and Aswan (upper Egypt, 23.9 N°, 32.9° E, 180 m elevation). Daily measured weather data were collected at the four field experiments by the Central Laboratory of Agricultural Climate (CLAC) in Egypt (www.clac.edu.eg) and used for specifying the range of wheat growing season mean temperature in each location. Based on the World Reference Base for Soil Resources, the main soil group along the river Nile is Fluvisols, and main texture is clay and loamy clay (FAO, 1998, Taha, 2000).

The field experiments were conducted using two of the most common modern cultivars (Misr2 and Misr1) and a standard cultivar (Sakha93) under full irrigation and high fertilization (180 kg N ha^{-1}). Cultivars were sown on two planting dates, 20 November, which was the date recommended by (MALR, 2003), and 30 November (late sowing), which provided a contrasting temperature regime at the same location.

Field experiment measurements included 50% anthesis date, physiological maturity date, grain yield, for all cultivars under both recommended and late planting dates. Determination of nitrogen content in oven dry samples was carried out using Kjeldahl method and the percentage of total nitrogen was converted to protein concentration by multiplying by a conversion factor of 5.7 for grains of wheat (Mossé *et al.*, 1985).

Italy experiment

Experiments were carried out in 2003/2004 and 2004/2005 at the experimental station in Ottava, Sardinia, Italy (41°N, 8°E, 80 m elevation). The soil at the site is a sandy-clay-loam of depth about 0.6 m overlaid on limestone (Xerochrepts), with an average nitrogen content of 0.76%, and a C:N (w:w) ratio of 12. The soil water content was 22.4% (w:w) at field capacity (-0.02 MPa), and 11.9% at -1.5 MPa. The climate is typically Mediterranean, with a long-term average annual rainfall of 538 mm. In 2003/2004, the first sowing was made on 20 November and the second on 16 February. In 2004/2005, the first sowing was made on 5 January and the second on 17 March. Nitrogen fertilizer was applied at sowing at 60 kg N ha^{-1} or 100 kg N ha^{-1} as urea and ammonium bi-phosphate, respectively. The cv. Claudio and cv. Creso analyzed in this study were part of a wider set of 20 cultivars. In both seasons, two adjacent fields were assigned to the two sowing dates and divided into three blocks. Within each block, nitrogen rate represented the main plots, and cultivars represented the sub-plots. Plots were 10 m^2. Sprinkler irrigation was used to ensure optimal growing conditions. Weeds, pests, and diseases were chemically controlled.

Anthesis (anthers exerted from the spikelets) and maturity (‘yellow peduncle stage’) (Chen *et al.*, 2010b) were timed when 50% of the ears in a plot reached the stage. At maturity, two 1 linear meter samples per plot from different rows were cut at the ground level, and then air-dried and weighed. Ears were separated from the rest of the sample, and then counted and threshed. Grain yield was calculated on a whole plot basis, following mechanical harvesting. Grain nitrogen concentrations were determined by the Kjeldhal method and the percentage of total nitrogen was converted to protein concentration by multiplying by a conversion factor of 5.7 for grains of wheat (Mossé *et al.*, 1985). More details about the experiments can be found in (Giunta *et al.*, 2007).

USA experiment

Two soft wheat advanced breeding lines, VA12W-72 developed by university of Virginia and GA06493-13LE6 developed by university of Georgia, and three standard cultivars, AGS2000, Jamestown, and USG3120, were planted at the plant science research and education unit in Citra (29.4° N, 82.2° W, 24 m elevation), FL on 15 December 2014. The experiment was laid out in a randomized complete block design with three replications at 6.9 m^2 plots (1.5 m × 4.6 m). The soil of the location is mostly sandy loam. Round-up® herbicide was applied 15 days before planting to control different narrow leaf weeds. Buctril® and Harmony® Extra were applied at 4 and 6 weeks after planting to control broad-leaf weeds. Prosaro® fungicide was applied three times (at 10, 13, and 15 weeks) to control foliar diseases such as leaf and stripe rust and Septoria leaf and glume blotch. NPK were applied at the rate of 5-10-15 kg ha^{-1} plus sulphur and micronutrients at the day of planting. Additionally, 36 kg N ha^{-1} was applied as top dress two times through irrigation during January and February. Irrigation was applied throughout the cropping cycle by using a central pivot irrigation system to avoid water stress. The experiment was machine harvested in the first week of June 2015. Days to anthesis were recorded as days from emergence at which 50% of plants in a plot flowered. Days to maturity were calculated as emergence at which 50% of peduncles turned yellow. A machine harvested sample from freshly harvested grains was collected and oven dried for 48 h, and dry weights were measured. The fresh and dry weight samples were used to adjust moisture percent and final yield. Grain filling rate was calculated as yield divided by the difference of days to maturity to days to anthesis.

The data on the same genotypes were collected from ten other locations, including Griffin (33.3° N, 84.3° W, 298 m elevation) and Plains (32.1° N, 84.4° W, 755 m elevation) in Georgia; Quincy (30.6° N, 84.6° W, 63 m elevation) in Florida; Warsaw (38.0° N, 76.8° W, 40 m elevation) and Blacksburg (37.2° N, 80.4° W, 633 m elevation) in Virginia; Winnsboro (32.1° N, 91.7° W, 22 m elevation) in

Louisiana; Knoxville (36.0° N, 84.2° W, 270 m elevation) in Tennessee; Farmersville (33.1° N, 96.2° W, 199 m elevation) in Texas; and Lexington (38.0° N, 84.5° W, 298 m elevation) in Kentucky. In general, soils of these locations were heavier (more clay) than Citra, Florida. Fertilizers were applied based on soil testing in those locations. Fall and spring applications of fertilizers were practiced. Chemicals were applied to control narrow and broad leaf weeds. The plots were machine harvested at maturity.

CIMMYT experiment

The fourth data set was the International Heat Stress Genotype Experiment (IHSGE) carried out by CIMMYT that included six temperature environments (Reynolds *et al.*, 1994). The IHSGE was a 4-year collaboration between CIMMYT and key national agricultural research system partners to identify important physiological traits that have value as predictors of yield at high temperatures (Reynolds *et al.*, 1994). Experimental locations were selected based on a classification of temperature and humidity during the wheat growing cycle. "Hot" and "very hot" locations were defined as having mean temperatures above 17.5 and 22.5°C, respectively, during the coolest month. "Dry" and "humid" locations were defined as having mean VPD above and below 1.0 kPa, respectively. The present study used data from four of the original 12 locations (i.e., two growing seasons in two Mexico locations, and one growing season in two locations in Egypt and Sudan) to represent a range of temperatures. Of the sixteen genotypes originally included in the experiment, two were selected for the present study (cv. Bacanora 88 as the modern cultivar and cv. Debeira as the standard cultivar). Variables measured in the experiment included days to 50% anthesis, days to physiological maturity, final grain yield. All experiments were well watered and fertilized with temperature being the most important variable.

Statistical analysis of model performance

Measured (y_i) and simulated ($\hat{y}_i$) grain yield, grain protein yield, and grain protein concentration were compared using the mean squared error (MSE):

$$RMSE = \sqrt{\frac{1}{n}\sum_{i=1}^{n}(y_i - \hat{y}_i)^2} \qquad (1)$$

The root mean squared relative error (RMSRE) was also calculated as an error metric scaled to the unit of the measurement as:

$$\mathrm{RMSRE} = 100 \times \sqrt{\frac{1}{n}\sum_{i=1}^{n}\left(\frac{y_i - \hat{y}_i}{y_i}\right)^2} \qquad (2)$$

To assess the model skill the Nash–Sutcliffe modeling efficiency (EF; (Nash & Sutcliffe, 1970)) was calculated:

$$\mathrm{EF} = 1 - \frac{\sum_{i=1}^{N}(y_i - \hat{y}_i)^2}{\sum_{i=1}^{N}(y_i - \overline{y})^2} = 1 - \frac{\mathrm{MSE}}{\mathrm{MSE}_{\overline{y}}} \qquad (3)$$

where $\overline{y}$ is the average over the y_i and $\mathrm{MSE}_{\overline{y}}$ is the MSE for the model that uses $\overline{y}$ as an estimator. EF is a skill measure that compares model MSE with the MSE of using the average of measured values as an estimator.

Results are given in Table S4.

Table S4. Model error and skill for grain yield, grain protein yield, and grain protein concentration for the INRA and the Australian FACE experiments for the median of the 32 (grain yield) or 18 (grain protein) wheat model ensembles. RMSE, root mean squared error; RMSRE, root mean squared relative error; EF, modeling efficiency. The values in parenthesis were calculated when also including the treatments used for model calibration.

Experiment	Grain dry mass yield			Grain N yield			Grain protein concentration		
	RMSE ($t\ ha^{-1}$)	RMSRE (%)	EF (-)	RMSE ($kg\ N\ ha^{-1}$)	RMSRE (%)	EF (-)	RMSE (% of grain yield)	RMSRE (%)	EF (-)
INRA	0.37	5.36	0.82	12.43	8.04	-0.08	0.82	7.73	0.55
	(0.42)	(6.09)	(0.70)	(14.52)	(9.36)	(-0.08)	(0.91)	(8.61)	(0.41)
AGFACE	1.88	44.04	0.51	7.18	25.59	0.51	3.23	17.77	-3.05
	(0.66)	(44.04)	(0.51)	(16.80)	(25.59)	(0.51)	(3.23)	(17.77)	(-3.05)

Global impact assessment

Model inputs for global simulations

To carry out the global impact assessment and exclusively focus on climate change, region-specific cultivars were used in all 60 locations. The cultivars for locations 31 to 60 were partly based on the cultivars for locations 1 to 30. Observed local mean sowing, anthesis, and maturity dates were supplied to modelers with qualitative information on vernalization requirements and photoperiod sensitivity for each cultivar (Supplementary Fig. S5-6). Modelers were asked to sow at the supplied sowing dates and calibrate their cultivar parameters against the observed anthesis and maturity dates by considering the qualitative information on vernalization requirements and photoperiod sensitivity.

For locations 1 to 30 sowing dates were fixed at a specific date. For locations 31 to 60, sowing windows were defined and a sowing rule was used. The sowing window was based on sowing dates reported in literature. For locations 41, 43, 46, 53, 54, and 59, sowing dates were not reported in literature and estimates from a global cropping calendar were used (Portmann *et al.*, 2010). The cropping calendar provided a month (the 15th of the month was used) in which wheat is usually sown in the region of the location. The start of the sowing window was the reported sowing date and the end of the sowing window was set two months later. Sowing was triggered in the simulations on the day after cumulative rainfall reached or exceeds 10 mm over a 5-day period during the predefined sowing window. Rainfall from up to 5 days before the start of the sowing window was considered. If these criteria were not met by the end of the sowing window, wheat was sown on the last day of the sowing window. Sowing dates were left unchanged for future scenarios.

For locations 35, 39, 47, 49, and 55 to 57 (Supplementary Table S5), anthesis dates were reported in the literature. For the remaining sites, anthesis dates were estimated with the APSIM-Wheat model. Maturity dates were estimated from a cropping calendar for sites 31 to 32, 37 to 38, 41 to 46, 49 to 54, and 58 to 59 (Supplementary Table S5) where no information from literature was available. For locations 31 to 60, observed grain yields from the literature (Supplementary Table S5) were provided to modelers with the aim to set up wheat models to have similar yield levels, as well as similar anthesis and maturity dates. No yields were reported for sites 49 and 56 (Supplementary Table S5), so APSIM-Wheat yields were estimated and used as a guide.

Locations 1 to 30 (no water or N limitations; Supplementary Table S5) were simulated using the same soil information from Maricopa, USA. Soil information for locations 31 to 60 (Supplementary Table S5) were obtained from a global soil database (Romero *et al.*, 2012). The soil closest to a location was used, but for locations 39 and 59 (Supplementary Table S5), soil carbon was decreased after consulting local experts.

Initial soil nitrogen was set to 25 kg N ha^{-1} NO_3-N and 5 kg N ha^{-1} NH_4-N per 100 cm soil depth and reset each year for locations 31 to 60. Initial soil water for spring wheat sown after winter at locations 31 to 60 was set to 100 mm PAW, starting from 10 cm depth until 100 mm was filled in between LL and DUL. The first 10 cm were kept at LL (see soil profiles) and reset each year. If wheat was sown after summer, initial soil water was set to 50 mm PAW, starting from 10 cm depth until 50 mm was filled in between LL and DUL. The first 10 cm were kept at LL (see soil profiles) and reset each year.

For locations 31 to 60, fertilizer rates were determined from (Gbegbelegbe *et al.*, 2017) except for site 59 (Ethiopia) where N fertilizer was set to 60 kg N ha^{-1}. Fertilizer rates were set low (20 to 50 kg N ha^{-1}) at locations 31 to 32, 48, 51, 53, 60; medium (60 kg N ha^{-1}) at locations 33 to 43, 45 to 47, 49 to 50, 52, 54, 57 to 59; and relatively high (100 to 120 kg N ha^{-1}) at locations 44, 55 to 56. All fertilizer was applied at sowing.

Table S5. Location, name and characteristics of the cultivars, sowing date (locations 1-30) or sowing window (locations (31-60), and mean anthesis and physiological maturity date for the 30 locations (1-30) from high rainfall or irrigated wheat regions and thirty locations from low rainfall (low input) regions (31-60) of the world used in this study.

						Cultivar							
Location number	**Country**	**Location**	**Latitude / longitude (decimal)**	**Elevation (m a.s.l)**	**Irrigation (Y/N)**	**Name**	**Growth habit [a]**	**Vernalization requirement [b]**	**Photoperiod sensitivity [b]**	**Sowing date or window**	**Mean 50%-anthesis date**	**Mean maturity date**	**Reference used for choosing anthesis date**
01	USA, NE	Maricopa	33.06 / -112.05	358	Y	Yecora Rojo	S	2	1	25 Dec.	5 Apr.	15 May	-
02	Mexico	Obregon	27.33 / -109.9	41	Y	Tacupeto C2001	S	2	2	1 Dec.	15 Feb.	30 Apr.	-
03	Mexico	Toluca	19.40 / -99.68	2,667	Y	Tacupeto C2001	S	2	2	10 May	5 Aug.	20 Sep.	-
04	Brazil	Londrina	-23.31 / -51.13	610	Y	Atilla	S	3	3	20 Apr.	10 Jul.	1 Sep.	-
05	Egypt	Aswan	24.10 / 32.90	193	Y	Seri M 82	S	3	2	20 Nov.	20 Mar.	30 Apr.	-
06	The Sudan	Wad Medani	14.40 / 33.50	413	Y	Debeira	S	3	2	20 Nov.	25 Jan.	25 Feb.	-
07	India	Dharwar	15.43 / 75.12	751	Y	Debeira	S	3	2	25 Oct.	15 Jan.	25 Feb.	-
08	Bangladesh	Dinajpur	25.65 / 88.68	40	Y	Kanchan	S	2	2	1 Dec.	15 Feb.	15 Mar.	-
09	The Netherland	Wageningen	51.97 / 5.63	12	N	Aminda	W	6	6	5 Nov.	25 Jun.	5 Aug.	-
10	Argentina	Balcarce	-37.75 / -58.3	122	N	Oasis	W	5	5	5 Aug.	25 Nov.	25 Dec.	-
11	India	Ludhiana	30.90 / 75.85	244	Y	HD 2687	S	1	1	15 Nov.	5 Feb.	5 Apr.	-

12	India	Indore	22.72 / 75.86	58	Y	HI 1544	S	0	1	25 Oct.	25 Jan.	25 Mar.	-
13	USA, WI	Madison	43.03 / -89.4	267	N	Brigadier	W	6	6	15 Sep.	15 Jun.	30 Jul.	-
14	USA, KS	Manhattan	39.14 / -96.63	316	N	Fuller	W	4	4	1 Oct.	15 May	01 Jul.	-
15	UK	Rothamsted	51.82 / -0.37	128	N	Avalon	W	3	3	15 Oct.	10 Jun.	20 Aug.	-
16	France	Estrées-Mons	49.88 / 3.00	87	N	Bermude	W	6	6	5 Oct.	31 May	15 Jul.	-
17	France	Orleans	47.83 / 1.91	116	N	Apache	W	5	4	20 Oct.	25 May	7 Jul.	-
18	Germany	Schleswig	54.53 / 9.55	13	N	Dekan	W	5	2	25 Sep.	15 Jun.	25 Jul.	-
19	China	Nanjing	32.03 / 118.48	13	N	NM13	W	4	4	5 Oct.	5 May	5 Jun.	-
20	China	Luancheng	37.53 / 114.41	54	Y	SM15	W	6	4	5 Oct.	5 May	5 Jun.	-
21	China	Harbin	45.45 / 126.46	118	Y	LM26	S	1	5	5 Apr.	15 Jun.	25 Jul.	-
22	Australia	Kojonup	-33.84 / 117.15	324	N	Wyallkatchem	S	2	4	15 May	5 Oct.	25 Nov.	-
23	Australia	Griffith	-34.17 / 146.03	193	Y	Avocet	S	2	4	15 Jun.	15 Oct.	25 Nov.	-
24	Iran	Karaj	35.92 / 50.90	1,312	Y	Pishtaz	S	2	2	1 Nov.	1 May	20 Jun.	-
25	Pakistan	Faisalabad	31.42 / 73.12	192	Y	Faisalabad-2008	S	0	2	15 Nov.	5 Mar.	5 Apr.	-
26	Kazakhstan	Karagandy	50.17 / 72.74	356	Y	Steklov-24	S	2	4	20 May	1 Aug.	15 Sep.	-
27	Russia	Krasnodar	45.02 / 38.95	30	Y	Brigadier	W	6	6	15 Sep.	20 May	10 Jul.	-
28	Ukraine	Poltava	49.37 / 33.17	161	Y	Brigadier	W	6	6	15 Sep.	20 May	15 Jul.	-
29	Turkey	Izmir	38.60 / 27.06	14	Y	Basri Bey	S	4	4	15 Nov.	1 May	1 Jun.	-
30	Canada	Lethbridge	49.70 / -112.83	904	Y	AC Radiant	W	6	6	10 Sept.	10 Jun.	25 July.	
31	Paraguay	Itapúa	-27.33 / -55.88	216	N	Based on Atilla	S	3	3	25 May – 25 Jul.	- [d]	15 Oct. [e]	(Ramirez-Rodrigues *et al.*, 2014)
32	Argentina	Santa Rosa	−36.37 / -64.17	177	N	Based on Avocet	S	2	4	5 Jun. – 5 Aug.	- [d]	15 Dec. [e]	(Asseng *et al.*, 2013)
33	USA, GA	Watkinsville	34.03 / -83.41	220	N	Based on Brigadier	W	6	6	25 Nov. – 25 Jan.	- [d]	22 Jun.	(Franzluebbers & Stuedemann, 2014)
34	USA, WA	Lind	47.00 / -118.56	522	N	Based on AC Radient	W	4	4	28 Aug. – 28 Oct.	- [d]	31 Jul.	(Al-Mulla *et al.*, 2009, Donaldson *et al.*, 2001, Schillinger *et al.*, 2008)
35	Canada	Swift Current	50.28 / -107.78	10	N	Based on Steklov-24	S	2	4	18 May. – 18 Jul.	16 Jul.	28 Aug.	(Hu *et al.*, 2015)

36	Canada	Josephburg	53.7 / -113.06	631	N	Based on Steklov-24	S	2	4	15 May. – 15 Jul.	- [d]	28 Aug.	(Izaurralde *et al.*, 1998)
37	Spain	Ventas Huelma	37.16 / -3.83	848	N	Based on Basri Bey	S	4	4	18 Dec. – 18 Feb.	- [d]	15 Jun. [e]	(Royo *et al.*, 2006)
38	Italy	Policoro	40.2 / 16.66	14	N	Based on Basri Bey	S	4	4	17 Nov. – 17 Jan.	- [d]	15 May [e]	(Steduto *et al.*, 1995)
39	Italy	Libertinia	37.5 / 14.58	267	N	Based on Basri Bey	S	4	4	26 Nov. – 26 Jan.	4 May	30 May	(Pecetti & Hollington, 1997)
40	Greece	Thessaloniki	41.08 / 22.15	36	N	Based on Basri Bey	S	4	4	15 Nov. – 15 Jan.	- [d]	22 Jun.	(Lithourgidis *et al.*, 2006)
41	Hungary	Martonvásár	47.35 / 18.81	113	N	Based on Apache	S	5	4	15 Nov. – 15 Jan. [c]	- [d]	15 Jun. [e]	(Berzsenyi *et al.*, 2000)
42	Romania	Alexandria	43.98 / 25.35	73	N	Based on Brigadier	W	6	6	7 Oct. – 7 Dec.	- [d]	15 Aug. [e]	(Cuculeanu *et al.*, 1999)
43	Bulgaria	Sadovo	42.13 / 24.93	154	N	Based on Brigadier	W	6	6	15 Oct. – 15 Dec. [c]	- [d]	15 Jul. [e]	(Islam, 1991)
44	Finland	Jokioinen	60.80 / 23.48	107	N	Based on Steklov-24	S	2	2	1 May – 1 Jul.	- [d]	15 Aug. [e]	(Rötter *et al.*, 2012)
45	Russia	Yershov	51.36 / 48.26	102	N	Based on Steklov-24	S	2	4	6 May – 6 Jul.	- [d]	15 Sep. [e]	(Pavlova *et al.*, 2014)
46	Kazakhstan	Altbasar	52.33 / 68.58	289	N	Based on Steklov-24	S	2	4	15 Mar. – 15 May [c]	- [d]	15 Sep. [e]	(Pavlova *et al.*, 2014)
47	Uzbekistan	Samarkand	39.70 / 66.98	742	N	Based on SM15	W	6	4	5 Nov. – 5 Jan.	7 May	5 Jul.	(FAO, 2010)
48	Morocco	Sidi El Aydi / Jemaa Riah	33.07 / -7.00	648	N	Based on Yecora	S	1	1	5 Nov. – 5 Jan.	- [d]	1 Jun.	(Heng *et al.*, 2007)
49	Tunisia	Nabeul / Tunis	36.75 / 10.75	167	N	Based on Pishtaz	S	2	2	1 Dec. – 1 Feb.	29 Mar.	15 Jun. [e]	(Latiri *et al.*, 2010)
50	Syria	Tel Hadya / Aleppo	36.01 / 36.56	263	N	Based on Pishtaz	S	2	2	20 Nov. – 20 Jan.	- [d]	15 Jun. [e]	(Sommer *et al.*, 2012)
51	Iran	Maragheh	37.38 / 46.23	1,472	N	Based on SM15	W	6	4	13 Oct. – 13 Dec.	- [d]	15 Jun. [e]	(Tavakkoli & Oweis, 2004)

52	Turkey	Ankara	39.92 / 32.85	895	N	Based on Fuller	W	4	4	1 Sep. – 1 Nov	- [d]	15 Jul. [e]	(Ilbeyi *et al.*, 2006)
53	Iran	Ghoochan / Quchan	37.66 / 58.50	1,555	N	Based on Pishtaz	S	2	2	15 Oct. – 15 Dec. [c]	- [d]	15 Jun. [e]	(Bannayan *et al.*, 2010)
54	Pakistan	Urmar	34.00 / 71.55	340	N	Based on Yecora	S	1	1	15 Nov. – 15 Jan. [c]	- [d]	15 May	(Iqbal *et al.*, 2005)
55	China	Dingxi	35.46 / 104.73	2,009	N	Based on Pishtaz	S	2	2	15 Mar. – 15 May.	15 Jun.	2 Aug.	(Huang *et al.*, 2008)
56	China	Xuchang	34.01 / 113.51	110	N	Based on Wenmai	W	4	4	10 Oct. – 10 Dec.	25 Apr.	1 Jun.	[f]
57	Australia	Merredin	-31.50 / 118.2	3000	N	Based on Wyalkatchem	S	2	4	15 May – 25 Jul.	5 Oct.	25 Nov.	(Asseng *et al.*, 1998)
58	Australia	Rupanyup / Wimmera	-37.00 / 143.00	219	N	Based on Avocet	S	2	4	1 May – 1 Jul.	- [d]	15 Nov. [e]	(van Rees *et al.*, 2014)
59	Ethiopia	Adi Gudom	13.25 / 39.51	2,090	N	Based on Debeira	S	2	4	15 Jun. – 15 Aug. [c]	- [d]	15 Dec. [e]	(Araya *et al.*, 2015)
60	South Africa	Glen / Bloemfontein	-28.95 / 26.33	1,290	N	Based on Wyalkatchem	S	2	4	15 May – 15 Jul.	- [d]	15 Nov.	(Singels & De Jager, 1991)

[a] S, spring type; W, winter type.

[b] Vernalization requirement and photoperiod sensitivity of the cultivars range from nil (0) to high (6).

[c] Sowing date estimated using global cropping calendar.

[d] See Figure S8.

[e] Maturity date estimated using global cropping calendar.

f Yan Zhu, personal communication, August 4, 2015.

1

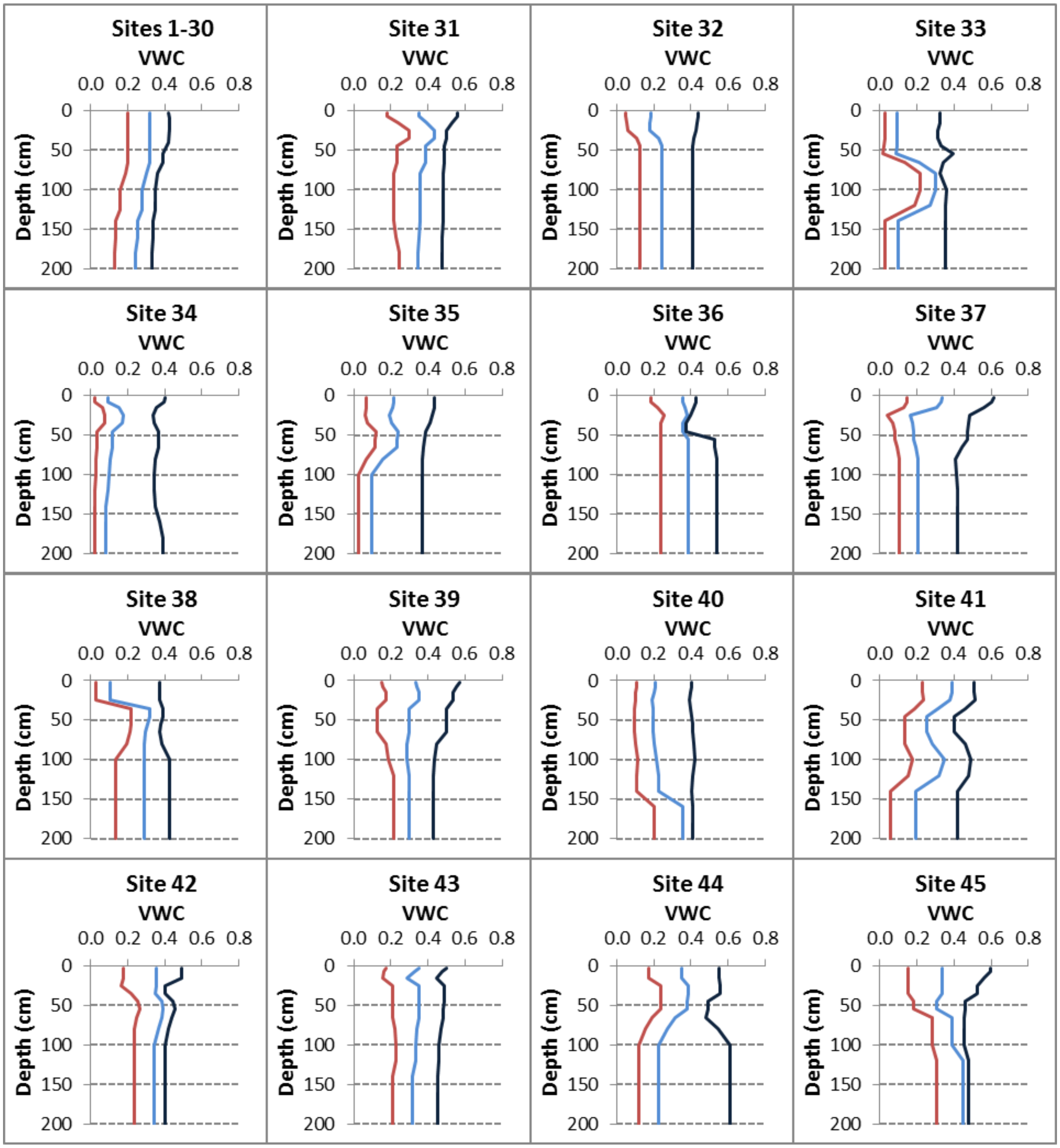

Fig. S1. Soil profile hydrological parameters used for locations 1 to 45. Changes in volumetric water content (VWC in v/v) with soil depth for characteristics water contents. The red line is the drained lower limit (-15 bar); the blue line is drained upper limit (field capacity); and the black line is saturated water content. The lower limit of crop water extraction was assumed to be the same as -15 bar lower limit.

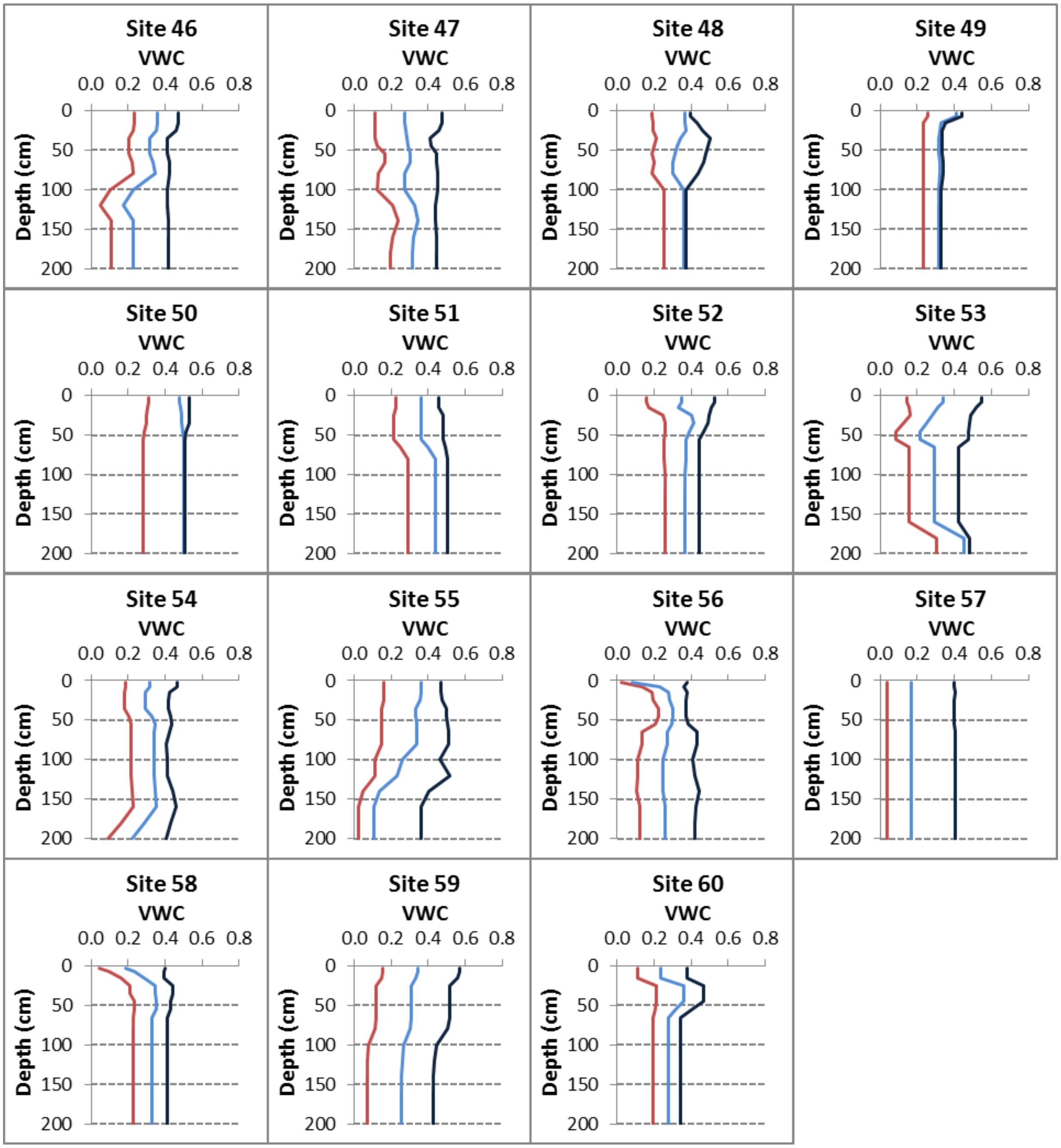

Fig. S2. Soil profile hydrological parameters used for locations 46 to 60. Changes in volumetric water content (VWC in v/v) with soil depth for characteristics water contents. The red line is drained lower limit (-15 bar); the blue line is drained upper limit; and the black line is saturated water content. The lower limit of crop water extraction was assumed to be the same as -15 bar lower limit.

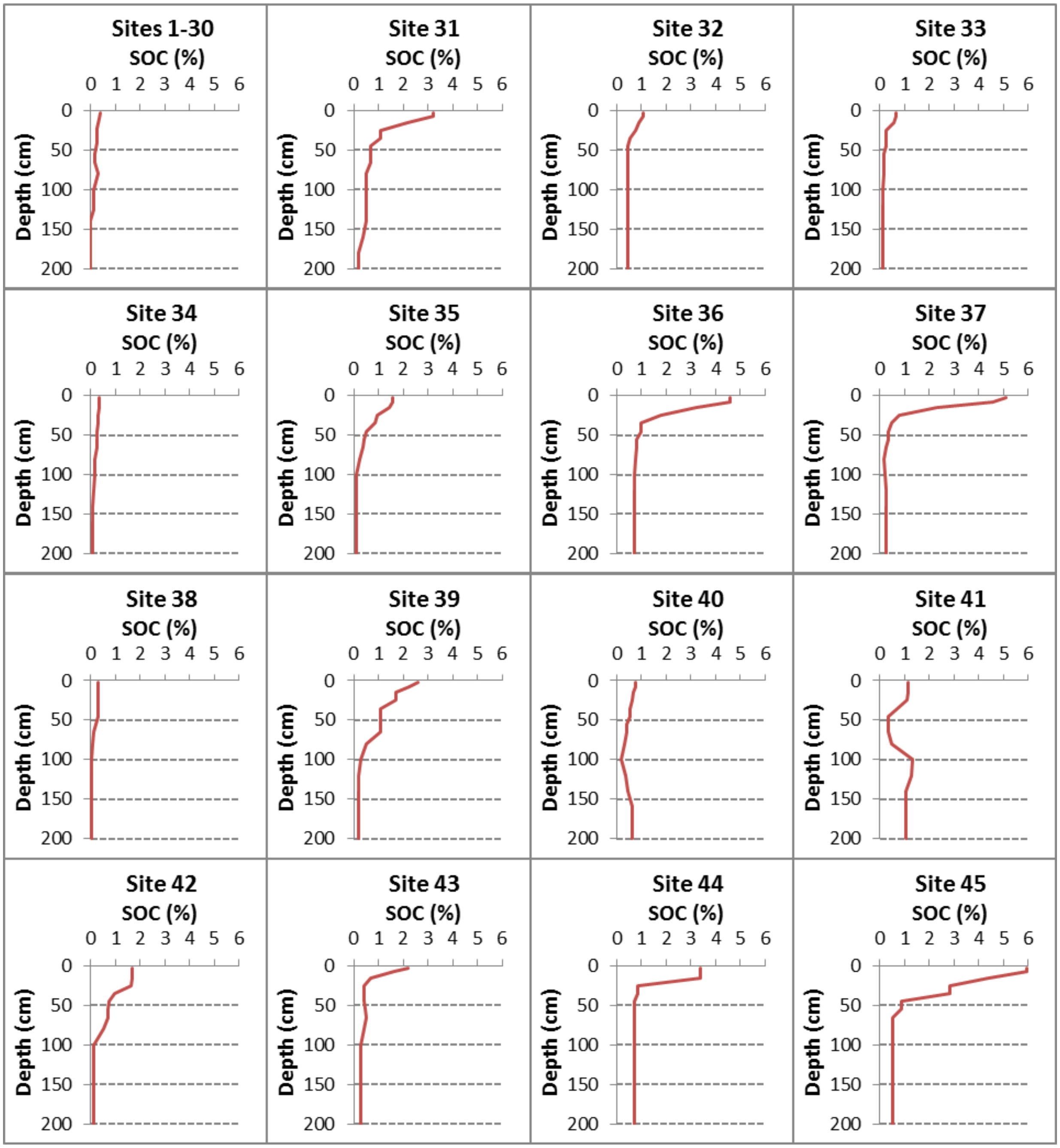

Fig. S3. Soil Organic Carbon (SOC) in different soil layers for locations 1 to 45.

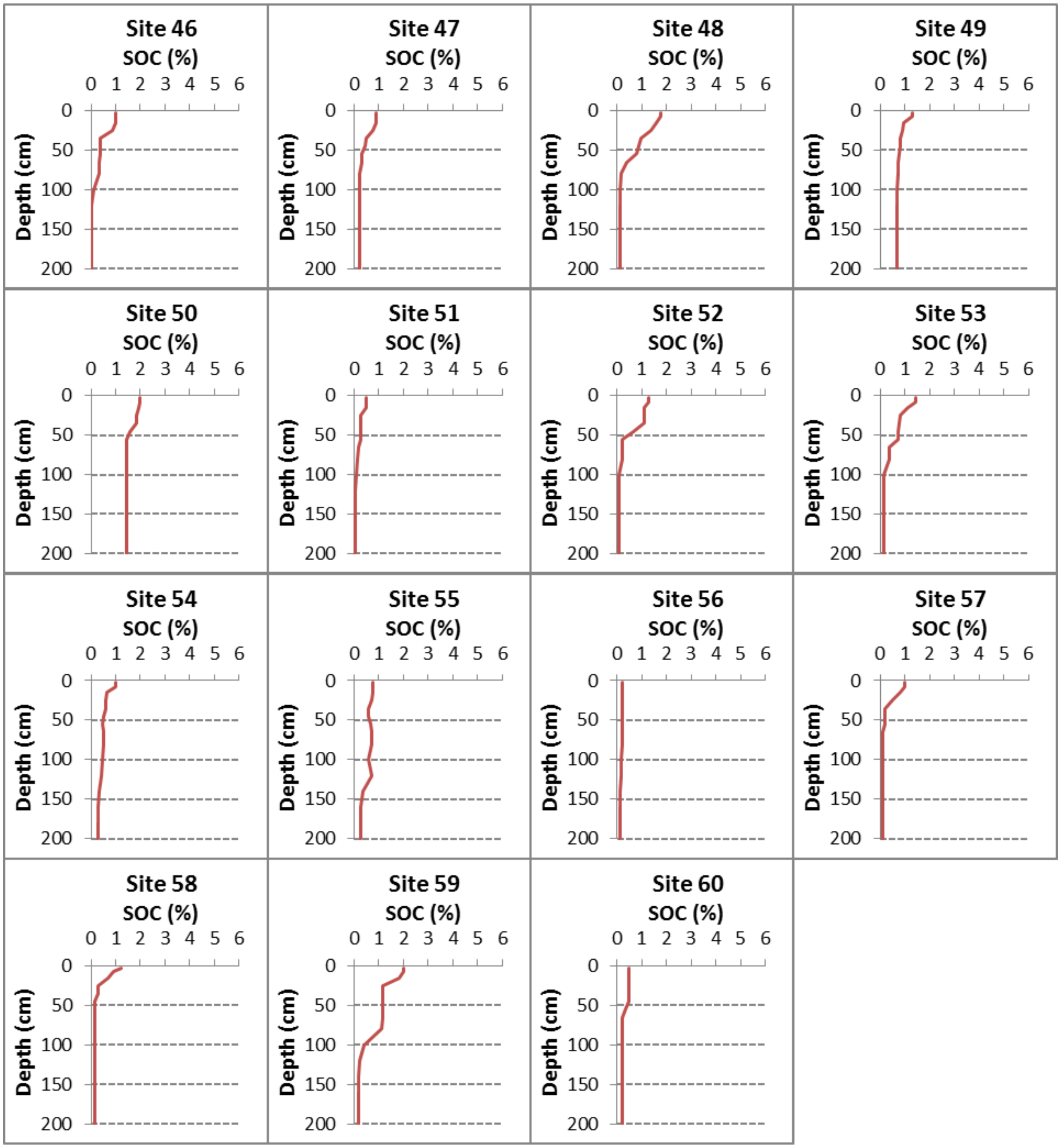

Fig. S4. Soil Organic Carbon (SOC) in different soil layers for locations 56 to 60.

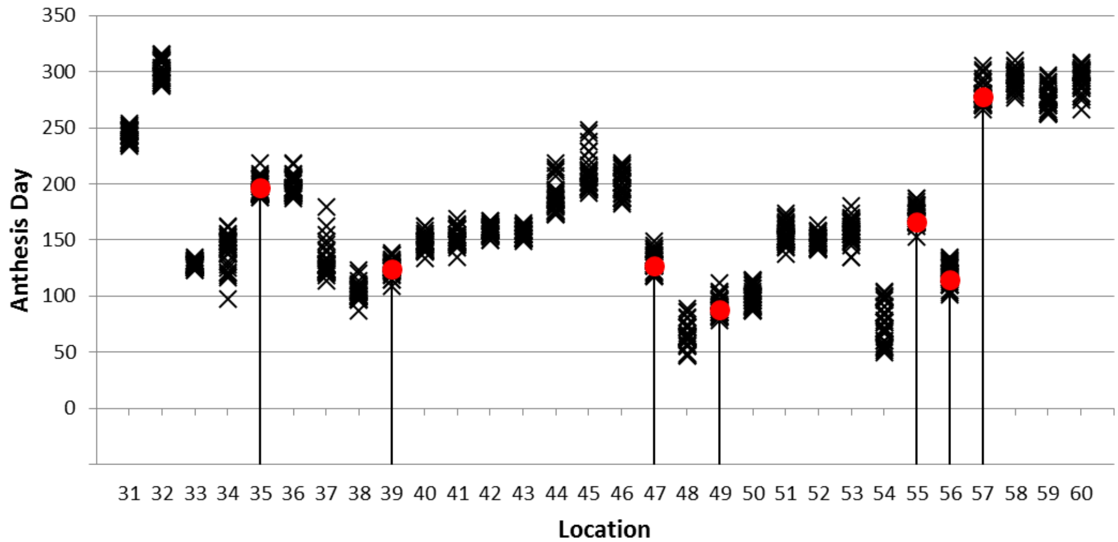

Fig. S5. Observed and simulated anthesis dates for location 31 to 60. Red dots are reported dates and black crosses are dates estimated by APSIM-Wheat model for years 1981-2010.

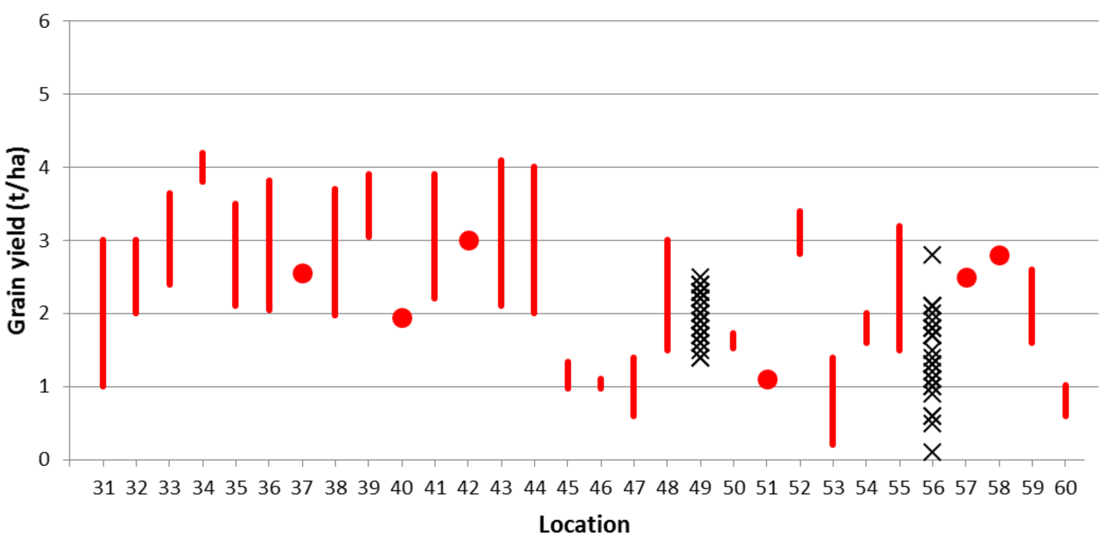

Fig. S6. Observed and simulated grain yields for locations 31 to 60. Red dots and lines show reported yield and yield ranges over several years, when available. Black crosses show grain yields simulated with the APSIM-Wheat model for locations 49 and 56 (1981-2010) where no observed yields were reported.

Future climate projections

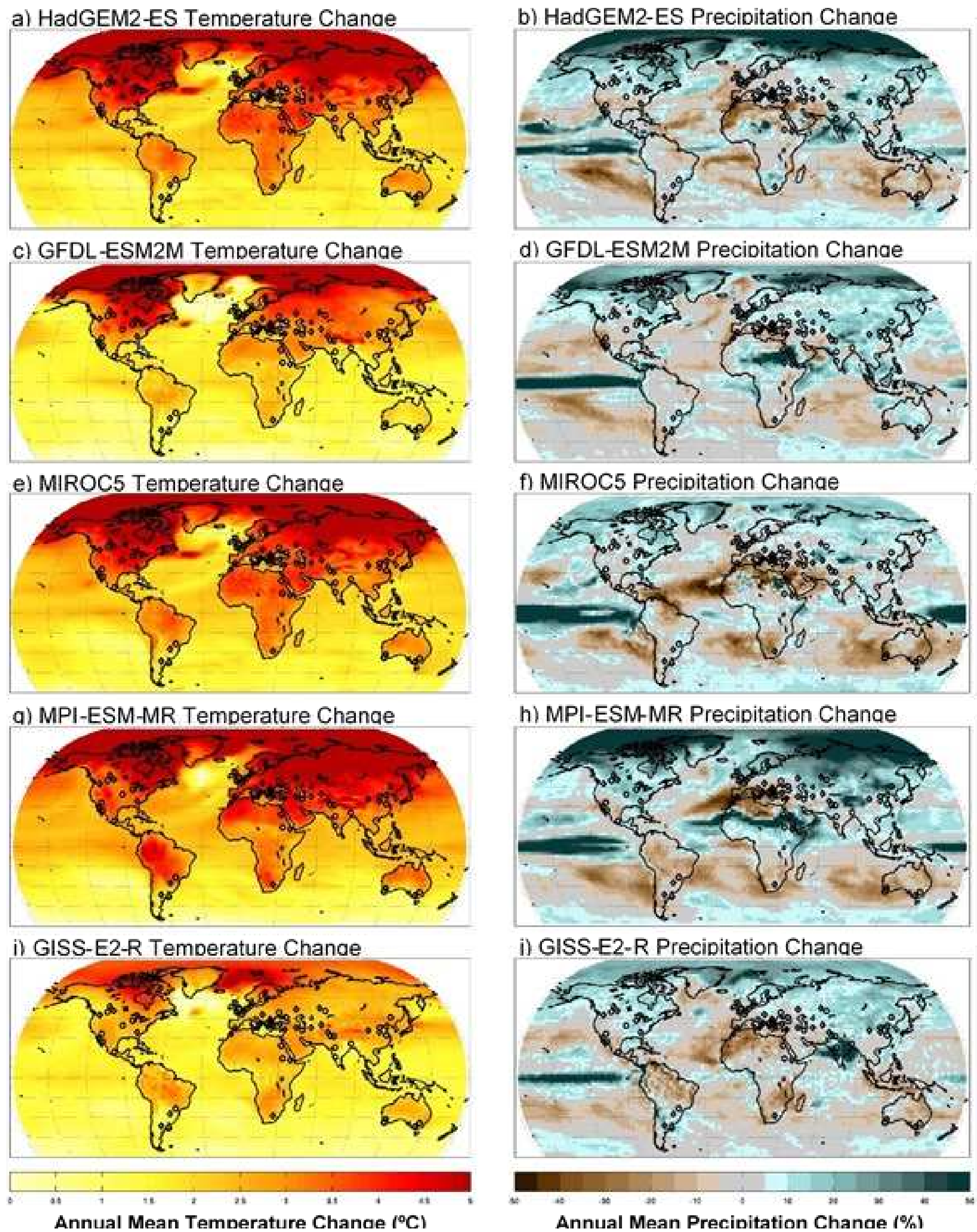

Fig. S7. Mean temperature and precipitation changes for the five GCMs used in this study. Mean annual RCP8.5 mid-century (2040-2069) temperature (left) and precipitation (right) changes compared to historical baseline (1980-2009) for the five selected GCMs. The locations of the 30 well-watered and 30 water-limited sites are noted as circles and diamonds, respectively.

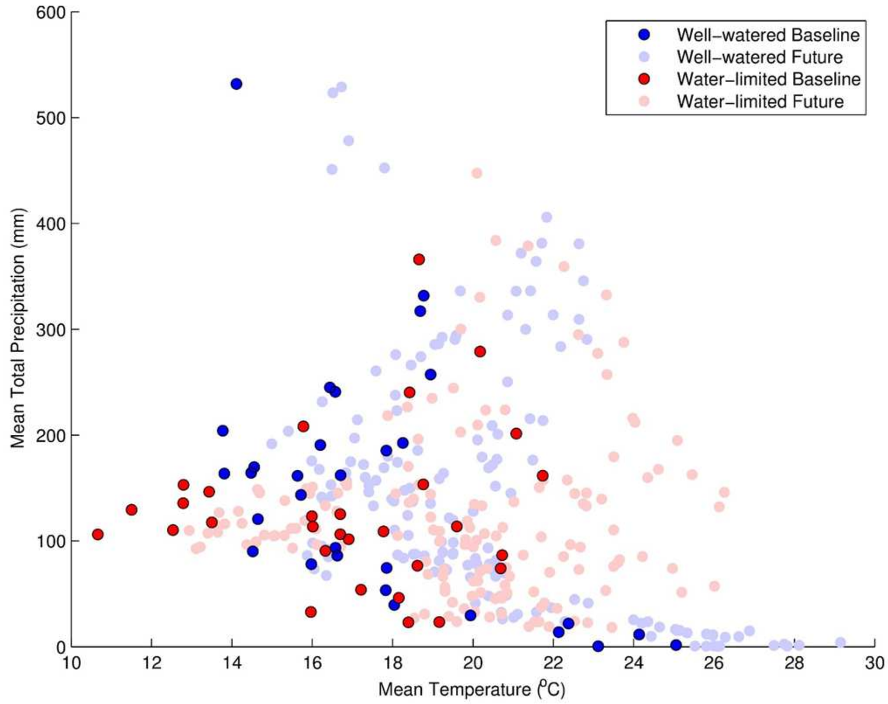

Fig. S8. Critical growing season climate for 60 wheat locations. Mean total precipitation versus mean temperature during the growing season for each the 30 high-rainfall or irrigated locations (well-watered) and 30 low rainfall (water-limited) for 1980-2010 (Baseline) and 2040-2069 (Future). Data for the future are for five GCM scenarios for RCP8.5.

Simulated adaptation

In 30 of the 32 models, anthesis date was delayed by increasing the thermal time requirement between emergence and anthesis, and for six models (AE, AF, DC, DN, OL, and WG) also by increasing the cold requirement and/or the photoperiod sensitivity. In two models (AE and DN) anthesis date was delayed without changing the thermal time requirement.

For the adaptation of grain filling trait, the 32 models were divided into five group according to how models incorporated the adaptation to increase grain filling rate.

Group 1: 17 models increased rate of grain filling (or HI change): AE, AF, AW, DN, EW, GL, IC, LI, MC, NC, NP, NS, OL, SA, MC, SS, ST, and WG.

Group 2: Five models with increased potential grain size (or final HI): CS, DC, DR, EI, and LP.

Group 3: Two models with increased fraction of vegetative biomass remobilization: L5 and SP.

Group 4: One model with decreased grain filling duration: AQ.

Group 5: Seven models with no parameter change to increase the rate of grain filling: DS, HE, MO, NG, S2, SQ, and WO.

The distributions of simulated grain yield with and without genetic adaptation under climate change the climate change scenarios for all 32 crop models and for the five groups were similar (Supplementary Fig. S9).

Table S6. Crop model parameters changed for adaptation to climate change. For each model the name, unit, definition, value of the parameters modified to delay anthesis date by 2 weeks and increase the rate of grain filling by 20% to adapt to climate change.

		Parameter			**Value** [a]	
Model name	**Trait**	**Name**	**Unit**	**Definition**	**Without adaptation**	**With adaptation**
APSIM-E	anthesis	Vern_sens	-	Vernalization sensitivity	1.61 [0.01-4.2]	2.81 [0.2-5]
	anthesis	photo_sens	-	Photoperiod sensitivity	1.62 [0.01-4.5]	2.98 [0.2-5]
	grain filling	potential_grain_filling_rate	mg/grain/d	Potential rate of grain filling	1.94 [1.5-3.0]	2.33 [1.8-3.6]
AFRCWHEAT2 [b]	anthesis	TT-EmAn	ºCd	Thermal time between emergence and anthesis	864 [531-1239]	1049 [794-1239]
	anthesis	Psat	h	Saturation photoperiod	14.4 [6-20]	15.2 [6-20]
	grain filling	GMAXGR	mg/grain/°Cd	Potential grain filling rate	0.074	0.089
AQUACROP	anthesis	GDDays: from sowing to anthesis	°Cd	Thermal time between sowing and anthesis	1428 [610-2100]	1673 [820-2400]
	grain filling	GDDays: building-up of Harvest Index during yield formation	°Cd	Thermal time for the building-up of harvest index during yield formation	929 [508-1478]	689 [280-1200]
APSIM-Wheat	anthesis	tt_end_juv	°Cd	Thermal time between end juvenile and floral initiation	380 [150-400]	462 [218-512]
	anthesis	tt_flor_init	°Cd	Thermal time between floral initiation and anthesis	534 [250-555]	651 [363-710]
	grain filling	potential_grain_filling_rate	mg/grain/d	Potential rate of grain filling	2.03	2.43
CropSyst	anthesis	Tteman	°Cd	Thermal time between crop emergence and anthesis	1581 [671-3318]	1327 [455-3020]
	grain filling	HI	-	Potential harvest Index	0.48	0.58
DSSAT-CERES-Wheat	anthesis	P1	°Cd	Thermal time between end juvenile and floral initiation	277 [140-460]	392 [250-500]
	anthesis	P1V	Vday	Optimum number of vernalizing days	30.3 [10-60]	31.5 [10-60]
	anthesis	P1D	%/10h	Photoperiod response	90 [10-200]	91 [10-200]
	grain filling	G2	mg/grain	Standard grain size under optimum conditions	40.3 [12-80]	48.3 [14-96]
DSSAT-Nwheat	anthesis	VSEN	°Cd	Vernalisation sensitivity	2.33 [1-5]	2.66 [1-5]
	anthesis	PPSEN	°Cd	Photoperiod sensitivity	2.45 [1-5]	4.11 [3-5]
	grain filling	MXFIL	mg/grain/d	Potential rate of grain filling	1.81 [1.4-2.5]	2.17 [1.68-3]

DSSAT-CROPSIM	anthesis	P1	°Cd	Thermal time from end juvenile to floral initiation	434 [350-500]	626 [450-750]
	grain filling	GWTS	mg/grain	Standard grain size under optimum conditions	37 [15-49]	44.4 [18-59]
DAISY	anthesis	DSRate1	DS/d	Development rate in the vegetative stage	0.029 [0.012-0.053]	0.023 [0.01-0.038]
	anthesis	DSeff	-	Development stage factor for assimilate production	1	1.2
EPIC-I	anthesis	PHU	°C	Thermal time between sowing and maturity	1688 [1000-2600]	2004 [1200-2800]
	grain filling	HI	-	Potential harvest index	0.45	0.54
EPIC-Wheat	anthesis	DLAI	-	Fraction of growing season when LAI declines	0.60	0.74 [0.69-0.84]
	grain filling	SCRP3	-	Development of harvest index relative to growing season	50.1	58.1
GLAM	anthesis	GCWSPLFL	°Cd	Thermal time between sowing and anthesis	1168 [755-2080]	1419 [987-2412]
	grain filling	DHDT	-	Rate of change in harvest index	0.00797 [0.0035-0.01]	0.00957 [0.0042-0.012]
HERMES	anthesis	Tsum3	°Cd	Thermal time between double ridge and heading	715 [170-1100]	775 [200-1155]
	anthesis	Tsum4	°Cd	Thermal time between heading and anthesis	187 [120-270]	348 [230-400]
INFOCROP	anthesis	TTVG	°Cd	Thermal time between emergence and anthesis	822 [450-1780]	1012 [625-1780]
	grain filling	GFRVAR	mg/grain/d	Potential rate of grain filling	1.32 [0.9-2.4]	1.58 [1.08-2.4]
LINTUL4	anthesis	TSUM1	°Cd	Thermal time between emergence and anthesis	1195 [490-2170]	1455 [710-2510]
	grain filling	PGRIG	mg/grain/d	Potential rate of grain filling	2.0	2.4
SIMPLACE<Lintul-5, SlimWater3,FAO-56,CanopyT,HeatStressHourly>	anthesis	vTSUM1	°Cd	Thermal time between emergence and anthesis	915 [460-1802]	1119 [633-2079]
	grain filling	vFRTDM	-	Proportion of vegetative biomass translocated to grains under optimum conditions	0.074 [0.05-0.09]	0.089 [0.06-0.108]
LPJmL	anthesis	phu	°Cd	Thermal time between emergence and maturity	1876 [1250-2920]	2151 [1395-3300]
	grain filling	hiopt	-	Potential harvest index	0.5	0.6

MCWLA-Wheat	anthesis	rmaxv2	-	Maximum development rate between terminal spikelet initiation and anthesis	0.0435 [0.022-0.0964]	0.0298 [0.0172-0.0554]
	anthesis	rmaxr	-	Maximum development rate between anthesis and maturity	0.0334 [0.0143-0.1182]	0.0401 [0.0172-0.1418]
	grain filling	Hidt	-	Rate of change in harvest index	0.4007 [0.3-0.5]	0.4808 [0.36-0.6]
MONICA	anthesis	Tsum3	°Cd	Thermal time between double ridge and begin anthesis	481 [210-900]	538 [220-1020]
	anthesis	Tsum4	°Cd	Thermal time between begin anthesis and begin grain filling	172 [120-200]	386 [320-400]
Expert-N-CERES	anthesis	PHINT	°Cd	Phyllochron	112 [71-140]	122 [81-150]
	anthesis	P1	°Cd	Thermal time between emergence and terminal spikelet	228 [100-430]	314 [190-525]
	grain filling	G2	mg/grain/d	Potential rate of grain filling	3 [2.9-3.5]	3.6 [3.4-4.2]
Expert-N-GECROS [c]	anthesis	MTDV	d	Minimum thermal days for vegetative phase	54 [22-98]	64 [29-99]
Expert-N-SPASS	anthesis	PDD1	d	Phenological development days between emergence and anthesis	39 [31-51]	48 [38-61]
	grain filling	G2	mg/grain/d	Potential rate of grain filling	2.5 [2.5-3.5]	3.1 [3-4.2]
Expert-N-SUCROS	anthesis	Tsum_1	°Cd	Thermal time between emergence and anthesis	1206 [700-2100]	1428 [900-2420]
	grain filling	G2	mg/grain/d	Potential rate of grain filling	2.5 [2.5-3.5]	3.1 [3-4.2]
OLEARY	anthesis	ANTHDL	°Cdh	Photothermal time between sowing and anthesis	11700 [2500-22278]	14446 [3625-25620]
	anthesis	BOOTDL	°Cdh	Photothermal time between stem extension and booting	5087 [2500-6500]	5173 [2500-6500]
	grain filling	GRMAX	mg/grain/d	Potential rate of grain filling	2.56 [2-2.9]	3.07 [2.4-3.48]
Sirius	anthesis	PHYLL	°Cd/leaf	Phyllochron	83 [70-126]	105 [70-149]
SALUS	anthesis	Phase 3	Phyllochrone	Phyllochronic duration of phase 3	4.5	6.5
	grain filling	krPGR	mg/grain/d	Potential rate of grain filling	2	2.4
SIMPLACE<Lintul-2,CC,Heat,CanopyT,Re-Translocation>	anthesis	AirTemperatureSumAnthesis	°Cd	Thermal time between emergence and anthesis	692 [400-2000]	781 [423-2302]
	grain filling	FRTDM	-	Proportion of vegetative biomass translocated to grains under optimum conditions	0.15	0.18
SiriusQuality	anthesis	P	°Cd/leaf	Phyllochron	113 [80-160]	143 [95-190]

SSM-Wheat	anthesis	bdSELBOT	d	Biological days between stem elongation and booting	10.9 [10.9-10.9]	24.2 [12.1-36.7]
	grain filling	PDHI	1/d	Rate of change in harvest index	0.014 [0.014-0.014]	0.0168 [0.0168-0.0168]
STICS	anthesis	STLEVDRP	°Cd	Thermal time between emergence and anthesis	906 [505-1745]	1125 [715-2050]
	grain filling	VITIRCARB	1/d	Rate of change in harvest index	0.0081	0.00972
WHEATGROW [d]	anthesis	TS	-	Thermal sensitivity	0.85 [0.58-1.81]	0.79 [0.5-1.81]
	anthesis	PS	-	Photoperiod sensitivity	0.000263 [0.0001-0.00054]	0.000268 [0.0001-0.00075]
	anthesis	IE	-	Intrinsic earliness	0.96 [0.58-1.2]	1.38 [0.2-1.95]
	grain filling	BFF	-	Basic filling factor	0.78 [0.45-1.2]	1.11 [0.65-1.75]
WOFOST	anthesis	TSUM1	°Cd	Thermal time between emergence and anthesis	1393 [520-2120]	1643 [740-2500]

[a] For genotypic parameters the mean, minimum and maximum values (between squared brackets) for the 60 locations are given.

[b] In order to reach maturity thermal time between anthesis and maturity was increased by 33% at one site (#44).

[c] In order to delay the anthesis date by two weeks the base temperatures and/or the curvature of the temperature response function for phenology were also changed at three sites (#5, 22 and 25).

[d] In order to reach maturity the grain filling heat tolerance sensitivity parameter (HTS) was also increased by 17 to 80% at three sites (#10, 26, and 45).

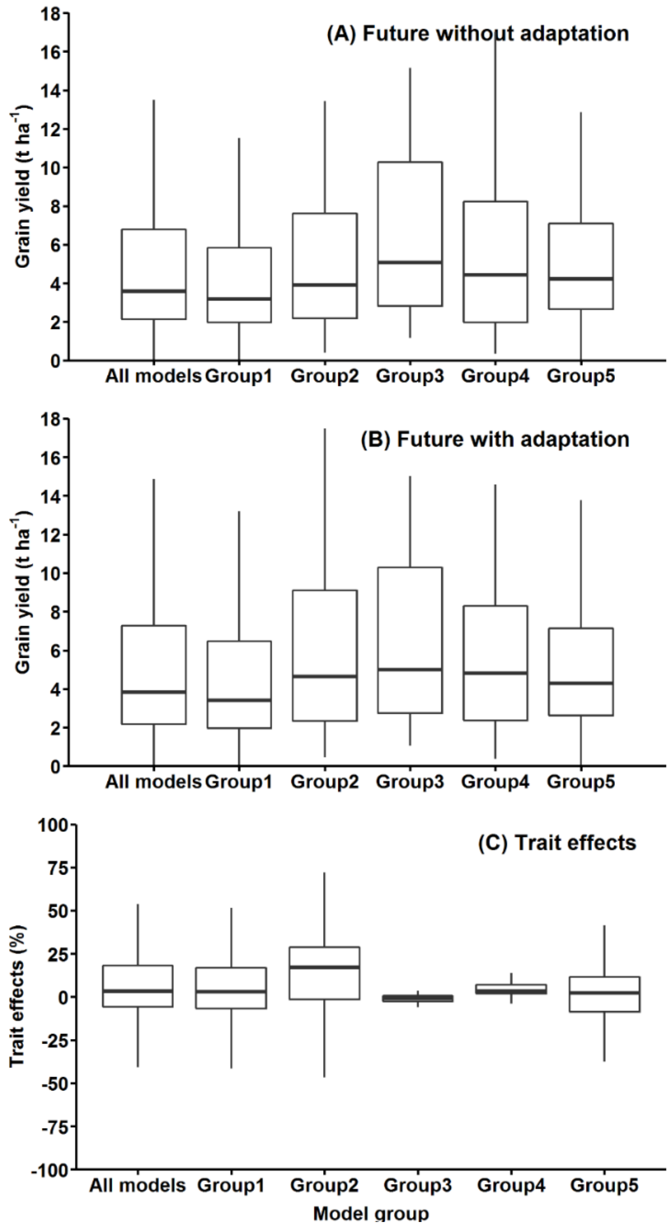

Fig. S9. Comparison of simulated absolute grain yield and genetic adaptation of grain yield for groups of crop models with different trait to increase grain filling rate. (**A**) Simulated yield distributions without adaptation, (**B**) simulated yield distributions with adaptation, and (**C**) distributions of simulated trait effects across the 60 global locations. All simulations are for 2040-2069 (RCP8.5, five GCMs). In each box plot, end of vertical lines represent from top to bottom, the 10^{th}, and 90^{th} percentiles, horizontal lines represent from top to bottom, the 25^{th}, 50^{th}, and 75^{th} percentiles of the simulations.

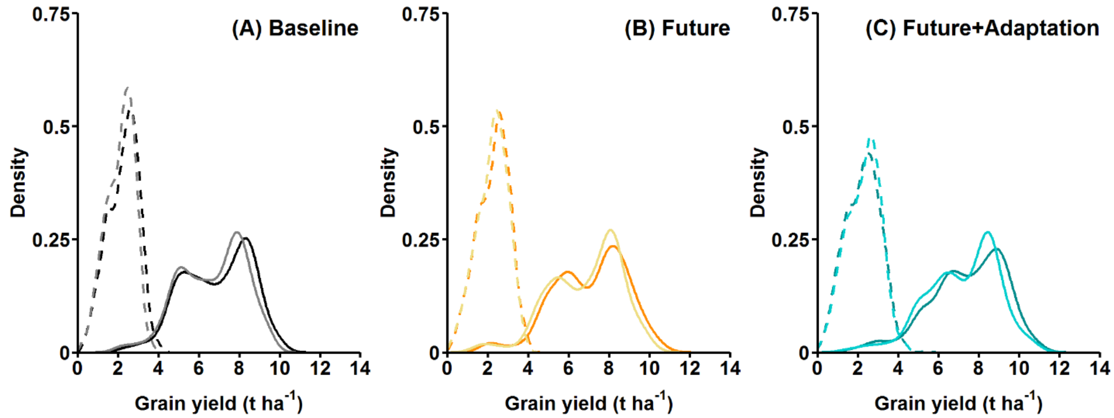

Fig. S10. Comparison of the distributions of simulated annual wheat grain yields from the 32-crop model ensemble median and the 18-crop model ensemble median used in grain protein simulations. (**A**) Baseline (grey: 18 models, black: 32 models); (**B**) climate change scenarios (light orange: 18 models, dark orange: 32 models); and (**C**) climate change scenario with genetic adaptation (light cyan: 18 models, dark cyan: 32 models) at rainfed (dash lines) and high rainfall or irrigated (solid lines) locations.

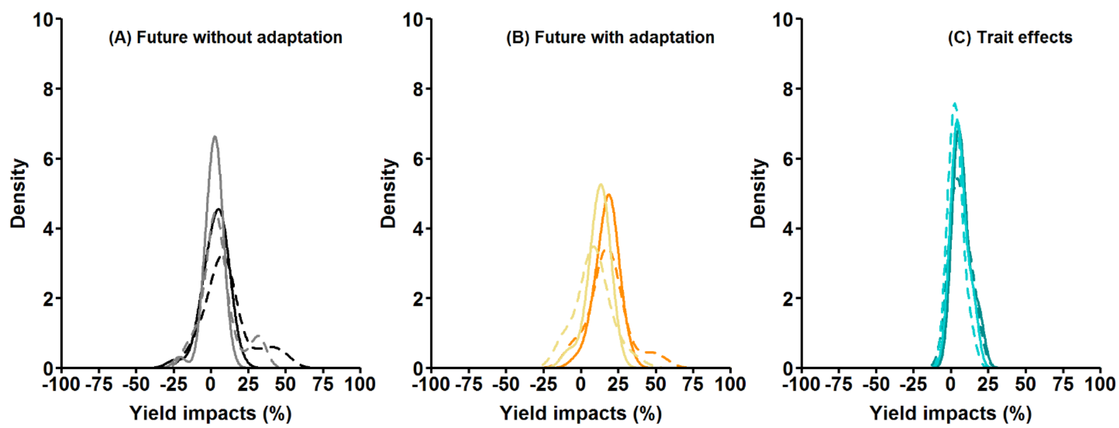

Fig. S11. Comparison of the distributions of simulated 30-year mean wheat yield impacts from the 32-crop model ensemble median and the 18-crop model ensemble median used in grain protein simulations. (**A**) Baseline (grey: 18 models, black: 32 models); (**B**) Future (light orange: 18 models, dark orange: 32 models); and (**C**) climate change scenario with genetic adaptation (light cyan: 18 models, dark cyan: 32 models) at rainfed (dash lines) and high rainfall or irrigated (solid lines) locations.

Table S7. Comparison of the distributions of simulated yield impacts of climate change without (Climate impacts) and with (Climate impacts + traits) genetic adaptation, and of genetic adaptation (Trait effects) for the 32 multi-model ensemble and the subset of 18 models used in the protein analysis. Impacts were calculated for 2040-2069 (RCP85, five GCMs) at the 30 low-rainfall or irrigated locations (Locations 1 to 30) and at the 30 low rainfall/input locations (Locations 31 to 60). Data are *P*-value from a Kolmogorov–Smirnov test.

Impacts	***P*-value [a]**	
	High rainfall or irrigated locations	**Low rainfall locations**
Climate impacts	0.07	0.07
Climate impacts + traits	< 0.01	< 0.01
Trait effects	0.81	0.24

[a] $P < 0.01$ indicates that the two distributions were significantly different.

Supplementary additional supporting results

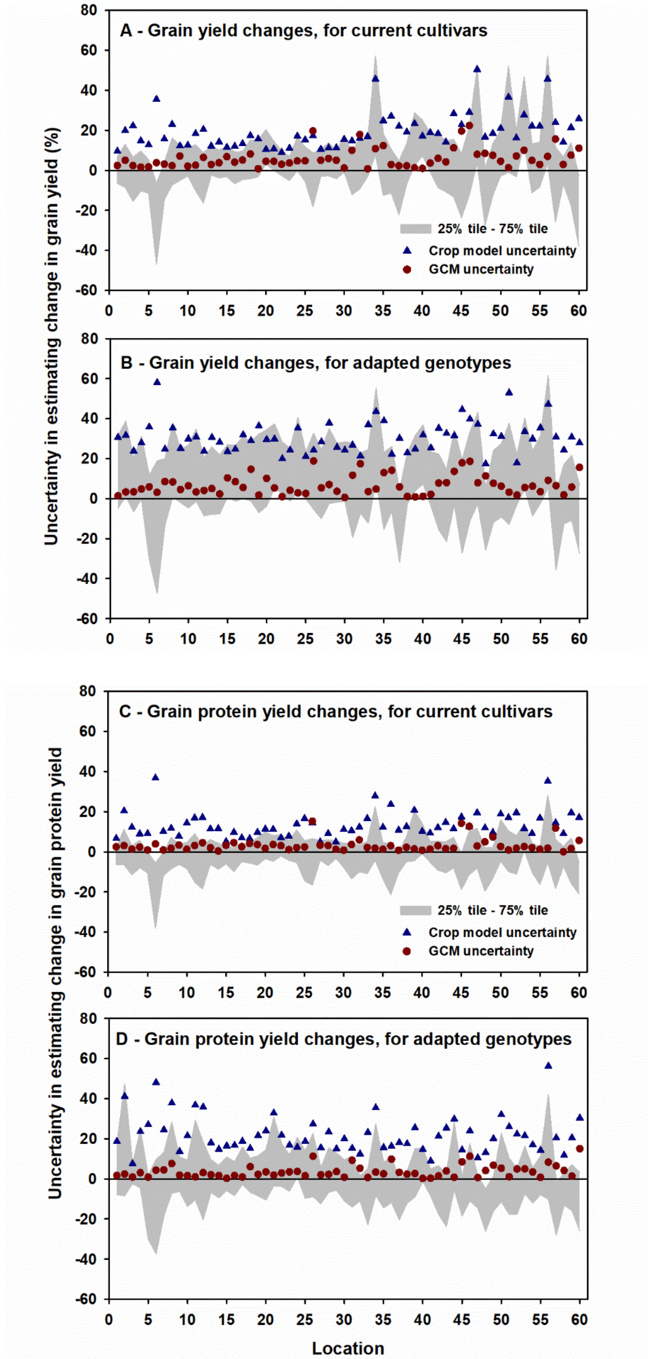

Fig. S12. Relative uncertainty (25th to 75th percentile) in estimating change in (**A** and **B**) grain yield and (**C** and **D**) grain protein yield, (**A** and **C**) with currently grown cultivars and (**B** and **D**) with adapted genotypes for crop models (triangle), GCMs (circles) and 25th to 75th percentile uncertainty range (grey shaded area) for crop models and GCM combined, based on a simulated multi-model ensemble projection under climate change of global wheat grain and protein yield for 2036-2065 under RCP8.5 compared with the 1981-2010 baseline across 32 models (or 18 for protein yield estimates) and five GCMs and the average over 30 years of yields using region-specific soils, cultivars and crop management. Locations are connected by line for uncertainty range (gray) to improve readability of this figure.

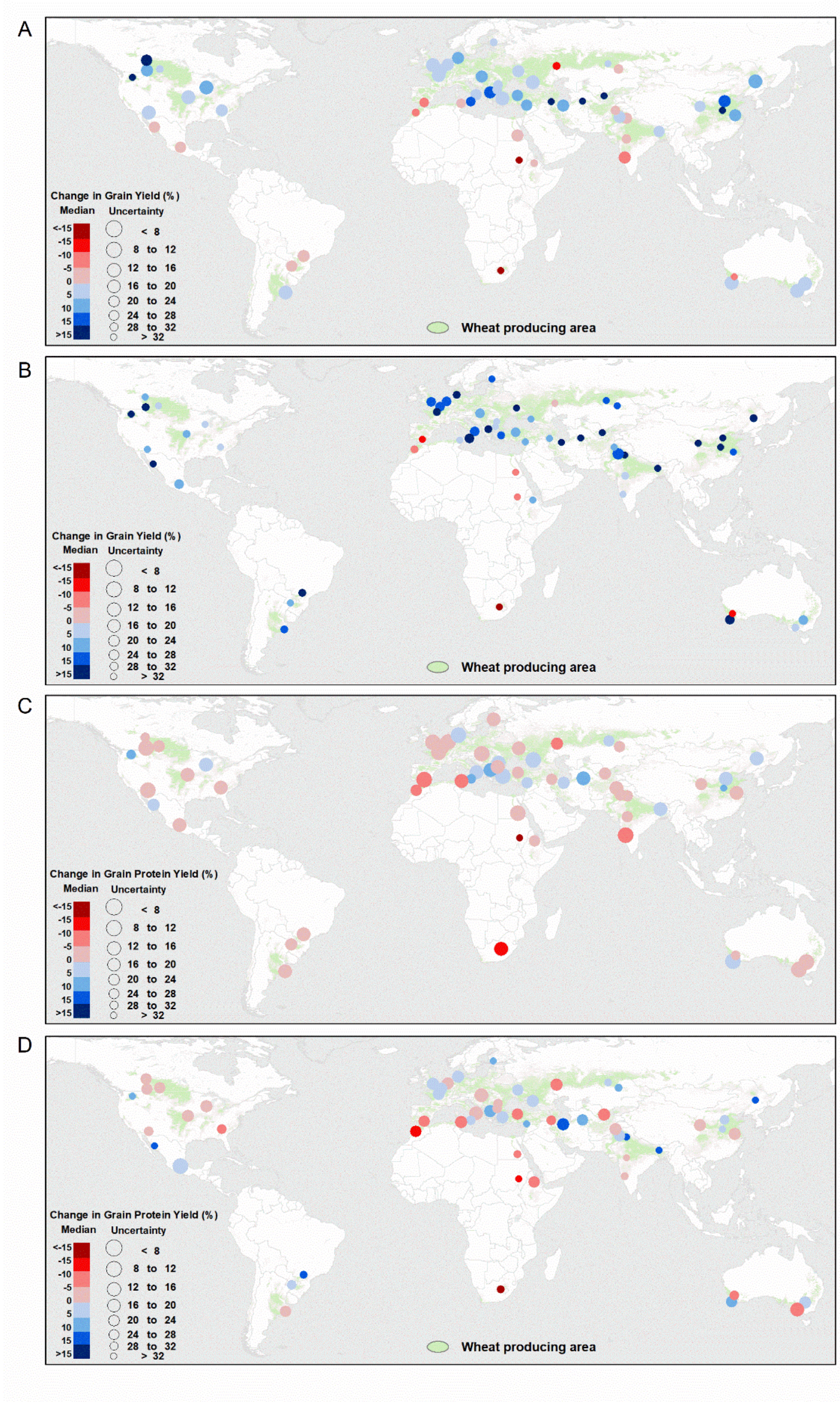

Fig. S13. Simulated global wheat grain and protein yield impacts from climate change with genotypic adaptation. Relative (**A** and **B**) grain yield and (**C** and **D**) grain protein yield impacts from climate change (**A** and **C**) without genetic adaptation and (**B** and **D**) with genetic adaptation for 2040-2069 (RCP8.5). Median across 32 crop models (18 for protein) and five GCMs and mean of 30 years using region-specific soils, cultivars, and crop management. Estimate of uncertainty (circle size) given as range between 25th and 75th percentiles for crop models and GCMs together. The larger the symbol, the higher the certainty.

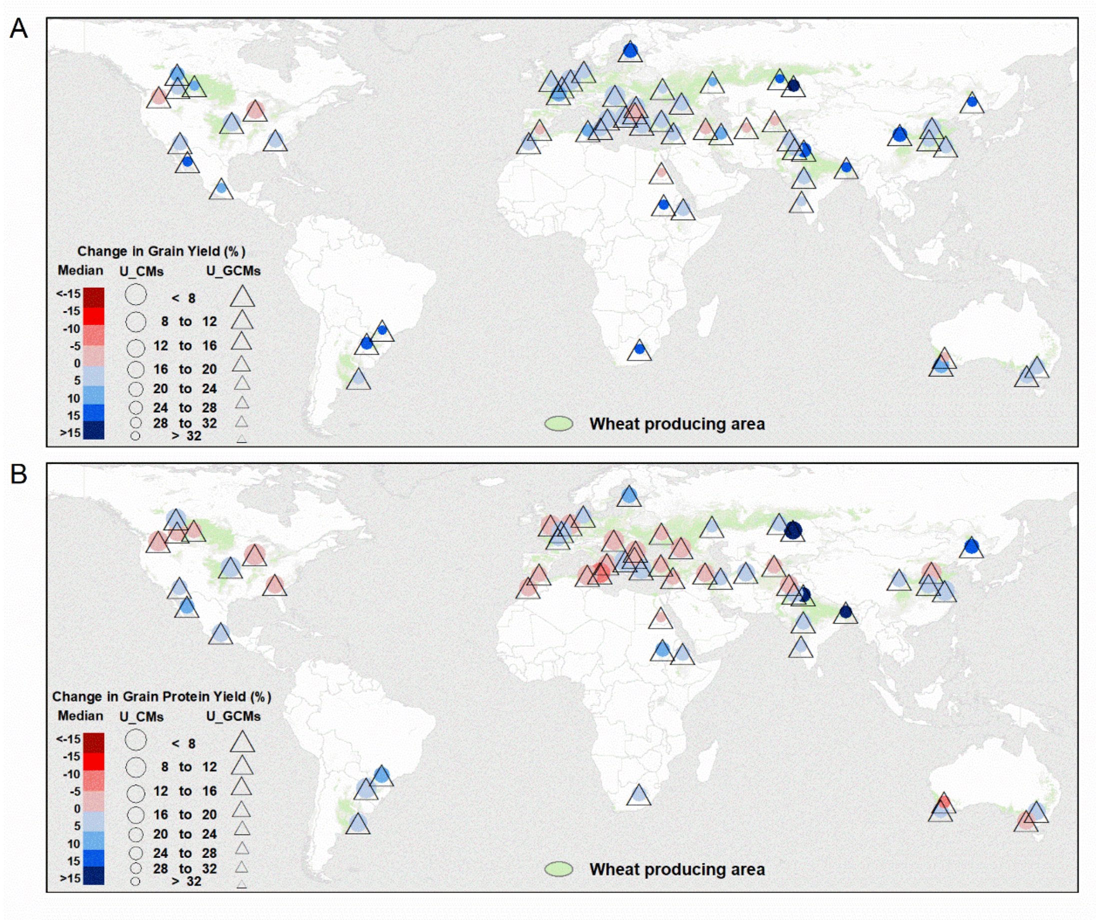

Fig. S14. Simulated trait effect for global wheat grain and protein yield. Relative effect of genetic adaptation on (**A**) grain yield and (**B**) grain protein yield for 2040-2069 (RCP8.5). Median across 32 crop models (18 for protein) and five GCMs and mean of 30 years using region-specific soils, cultivars, and crop management. Estimate of uncertainty given as range between 25th and 75th percentiles for crop models (circle size) and GCMs (triangle size). The larger the symbol, the less the uncertainty.

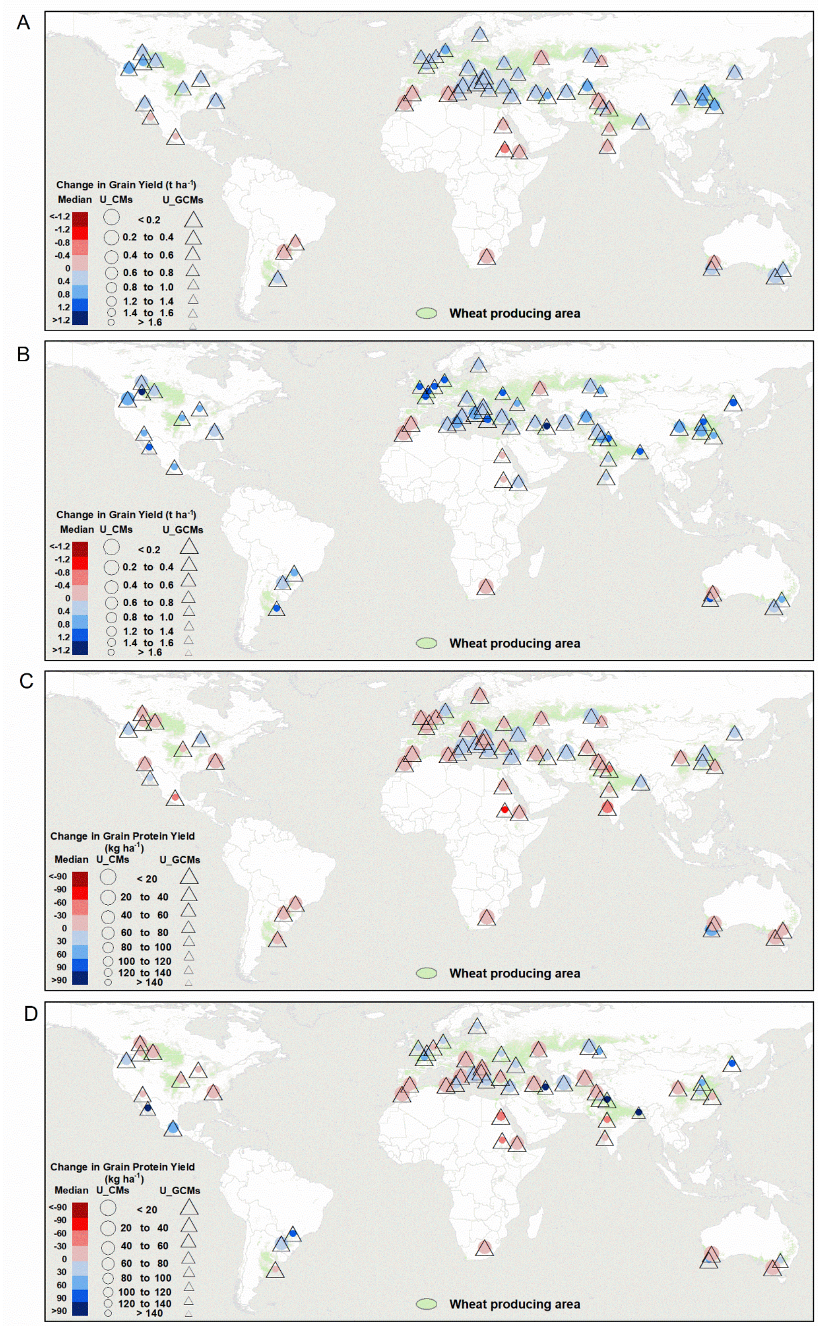

Fig. S15. Simulated global wheat grain and protein yield impacts from climate change with genotypic adaptation. Absolute (**A** and **B**) grain yield and (**C** and **D**) grain protein yield impacts from climate change (**A** and **C**) without genetic adaptation and (**B** and **D**) with genetic adaptation for 2030-2069 (RCP8.5). Median across 32 crop models (18 for protein) and five GCMs and mean of 30 years using region-specific soils, cultivars and crop management. Estimate of uncertainty given as range between 25th and 75th percentiles for crop models (circle size) and GCMs (triangle size). The larger the symbol, the higher the certainty.

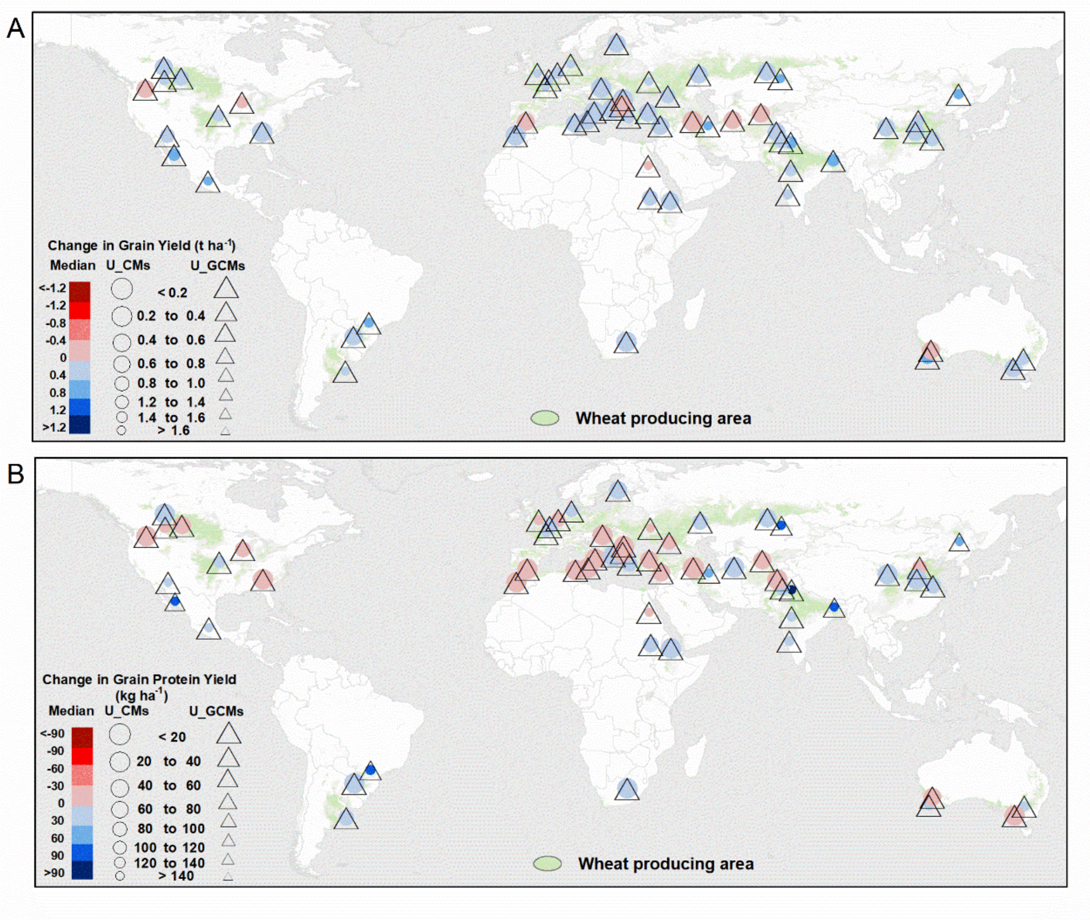

Fig. S16. Simulated trait effect for global wheat grain and protein yield. Absolute (**A**) grain yield and (**B**) grain protein trait effect for 2040-2069 (RCP8.5). Median across 32 crop models (18 for protein) and five GCMs and mean of 30 years using region-specific soils, cultivars, and crop management. Estimate of uncertainty given as range between 25th and 75th percentiles for crop models (circle size) and GCMs (triangle size). The larger the symbol, the less the uncertainty.

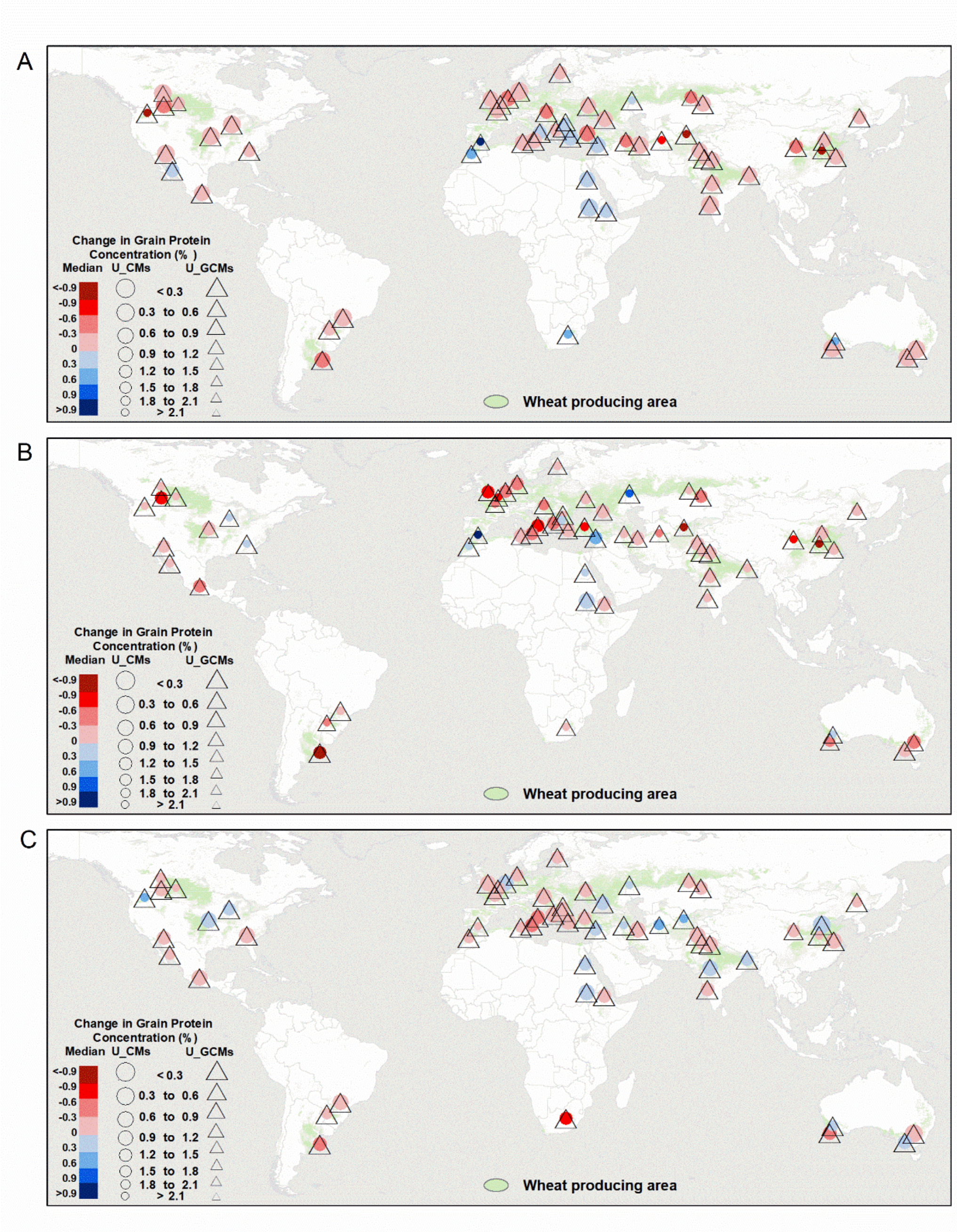

Fig. S17. Simulated global wheat grain protein concentration impacts from climate change with genotypic adaptation. Absolute grain protein concentration impacts from climate change (**A**) without genetic adaptation and (**B**) with genetic adaptation and (**C**) absolute traits effects for 2040-2069 (RCP8.5). Median across 18 crop models and five GCMs and mean of 30 years using region-specific soils, cultivars, and crop management. Estimate of uncertainty given as range between 25^{th} and 75^{th} percentiles for crop models (circle size) and GCMs (triangle size). The larger the symbol, the higher the certainty.

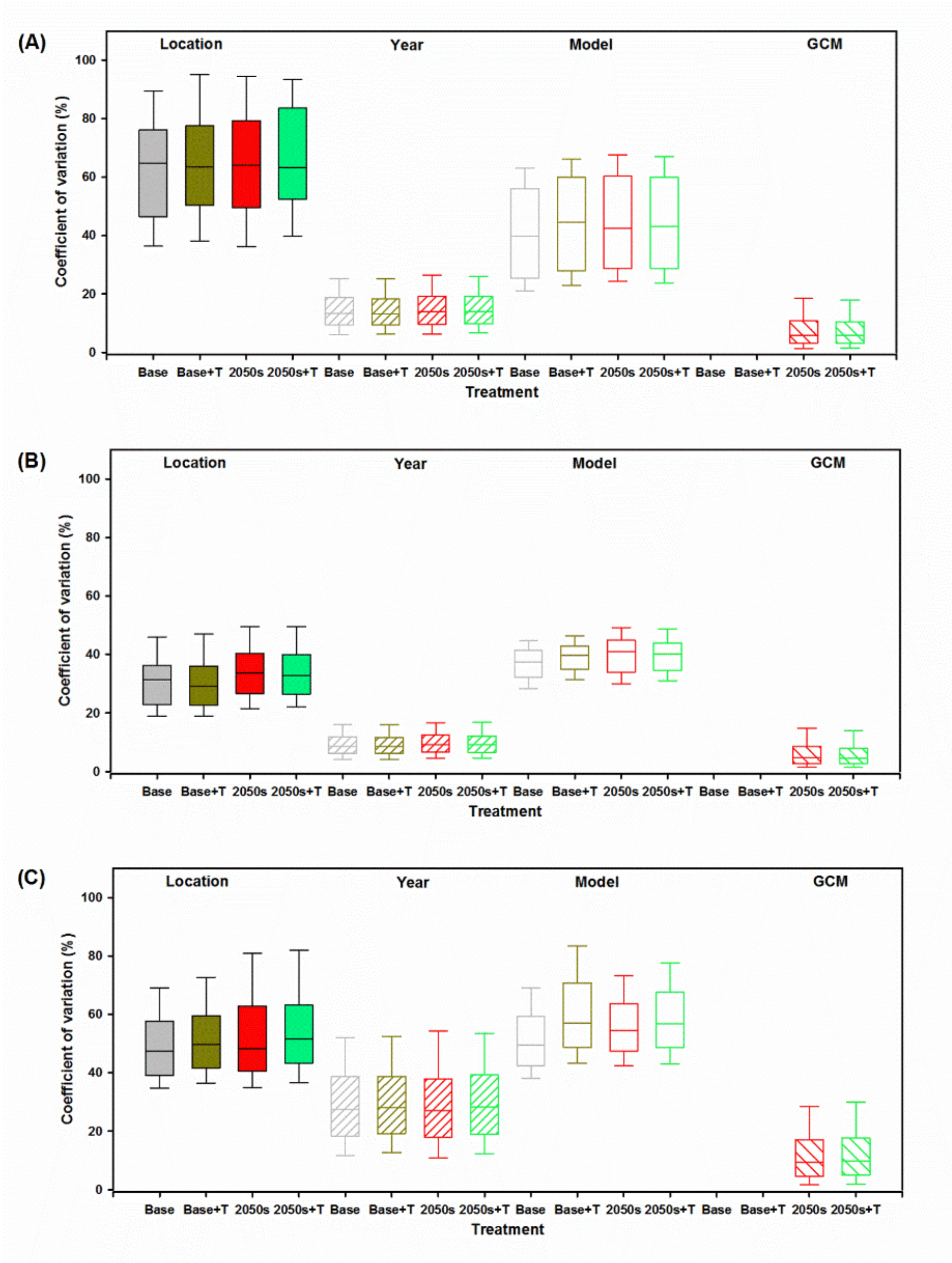

Fig. S18. Coefficient of variability of simulated wheat grain yields. (**A**) all 60 locations, (**B**) the 30 high rainfall or irrigated locations, and (**C**) the 30 low rainfall locations based on 32 crop models, five GCMs, and 30 years for baseline (Base), baseline with genetic adaptation (Base+T), climate change scenarios from 5 GCMs for 2040-2069 (RCP8.5) without genetic adaptation (2050s) and with genetic adaptation (2050s+T). In each box plot, horizontal lines represent from top to bottom, the 10^{th}, 25^{th}, 50^{th}, 75^{th}, and 90^{th} percentiles of the simulations.

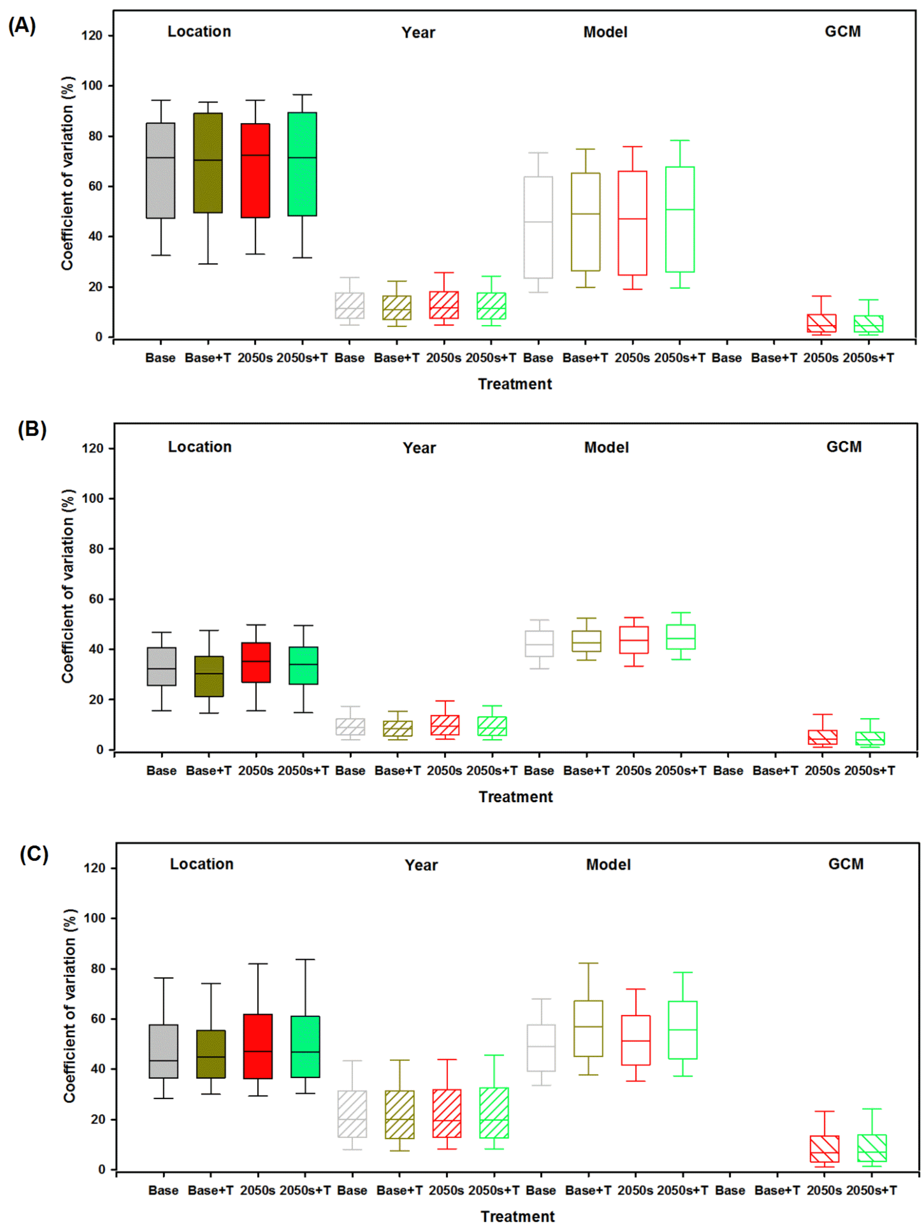

Fig. S19. Coefficient of variability of simulated wheat grain protein yields for (**A**) 60 locations, (**B**) for the high rainfall and irrigated locations, and (**C**) for low rainfall locations, based on 18 crop models, 5 global climate models (GCMs), 30 years. (**A**) 60 locations and (**B**) 30 high rainfall/irrigated locations and (**C**) 30 low rainfall locations for baseline (Base), baseline plus traits (Base+T), climate change scenario for 2050s (RCP8.5) without traits (2050s) and with traits (2050s+T), In each box plot, horizontal lines represent from top to bottom, the 10th, 25th, 50th, 75th, and 90th percentiles of the simulations.

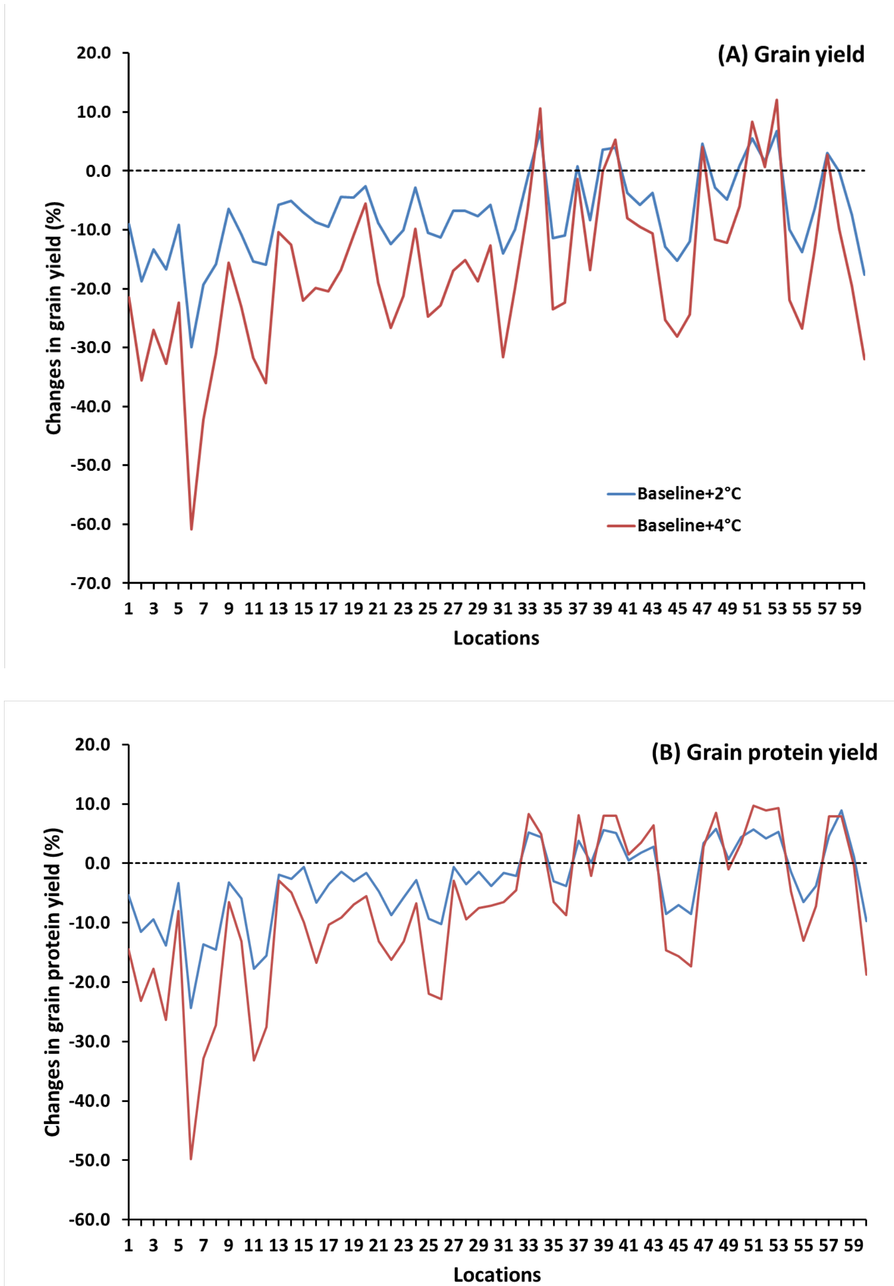

Fig. S20. Simulated wheat grain and protein yield impacts from increasing temperatures. Relative change in (**A**) grain yield and (**B**) for grain protein yield in response to a temperature increase of 2°C (Baseline+2ºC) or 4°C (Baseline+4ºC) for the baseline period (1981-2010) under historical CO_2 concentration (360 ppm) at the 60 global locations (locations 1 to 30 are irrigated or high rainfall and locations 31 to 60 are rainfed/low input; see Table S5 for details of the locations). Data are ensemble median for 32 crop models (18 for protein) and mean of 30 years using region-specific soils, cultivars, and crop management. Locations are connected by line to improve readability of this figure.

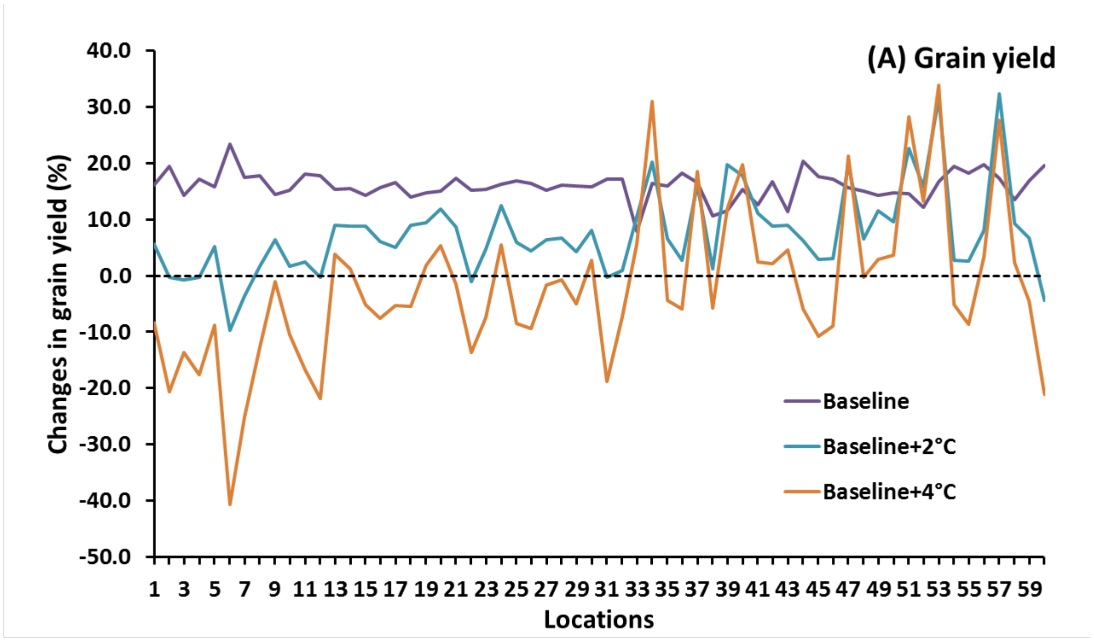

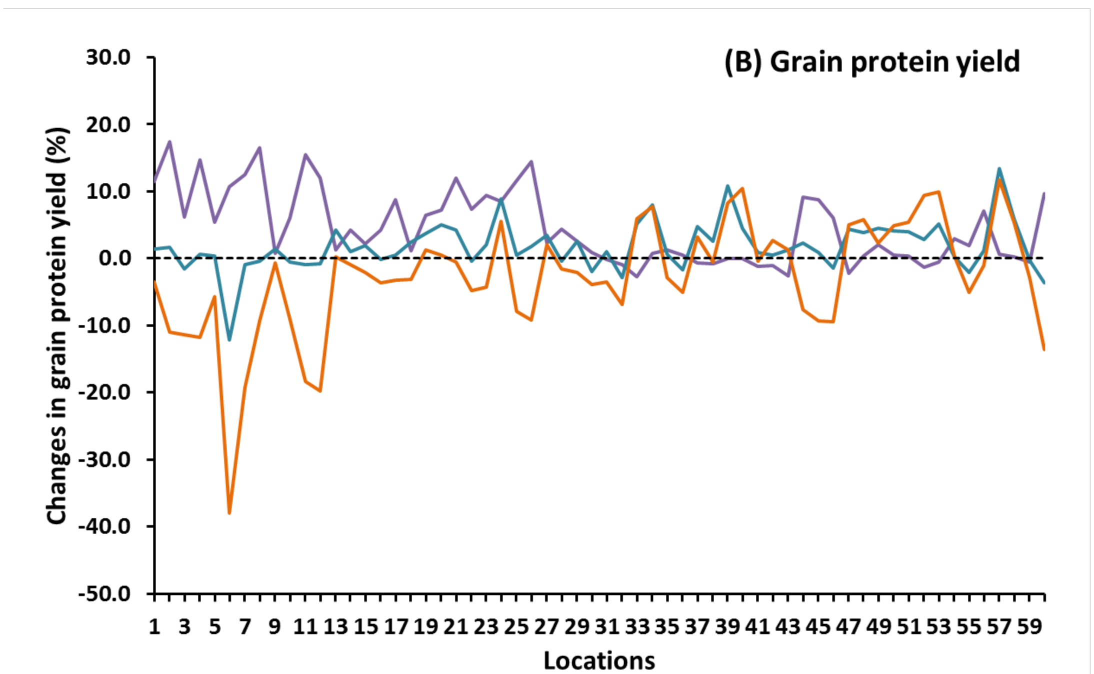

Fig. S21. Simulated wheat grain and protein yield impacts from elevated CO_2. Relative response to CO_2 (360 vs. 550 ppm) for (**A**) grain yield and (**B**) for grain protein yield for the baseline period (1981-2010; Baseline) and for the baseline period with a temperature increase of 2°C (Baseline+2ºC) or 4°C (Baseline+4ºC) at the 60 global locations (locations 1 to 30 are irrigated or high rainfall and locations 31 to 60 are rainfed/low input; see Table S5 for details of locations). Data are ensemble median for 32 crop models (18 for protein) and mean of 30 years using region-specific soils, cultivars, and crop management. Locations are connected by line to improve readability of this figure.

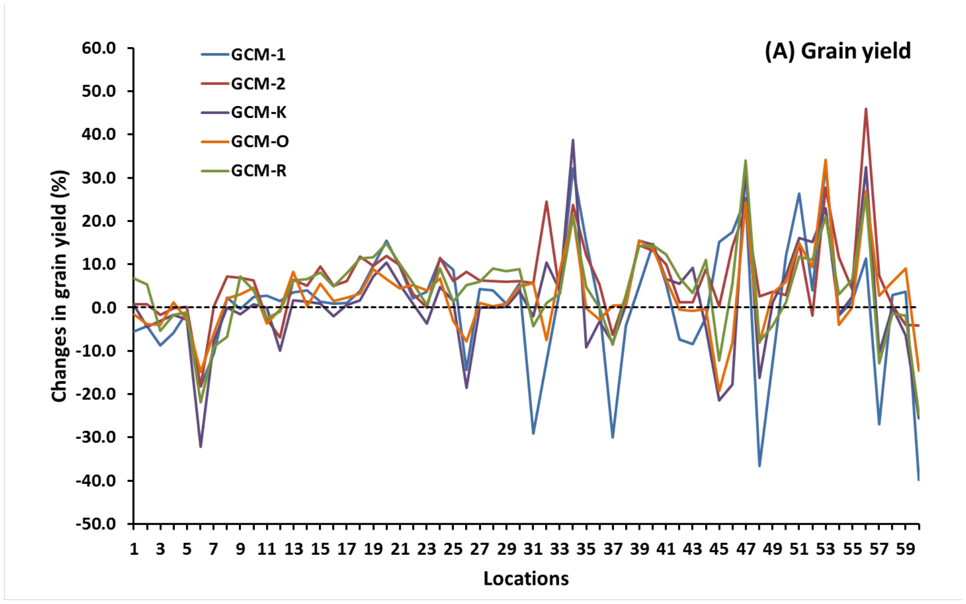

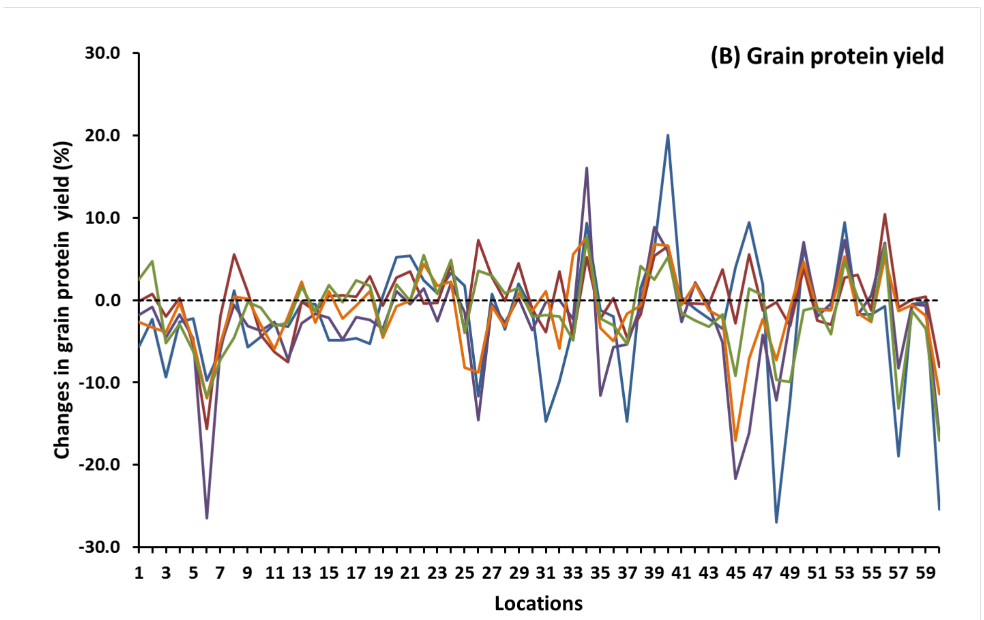

Fig. S22. Simulated wheat grain and protein yield impacts with climate change under five global climate models (GCMs) without genetic adaptation. Relative (**A**) grain yield and (**B**) grain protein yield impact for five GCMs for 2040-2069 (RCP8.5) at the 60 global locations (locations 1 to 30 are irrigated or high rainfall; locations 31 to 60 are rainfed/low input; see Table S5 for details of the locations). Data are ensemble median for 32 crop models (18 for protein), and mean of 30 years using region-specific soils, cultivars and crop management. Locations are connected by line to improve readability of this figure.

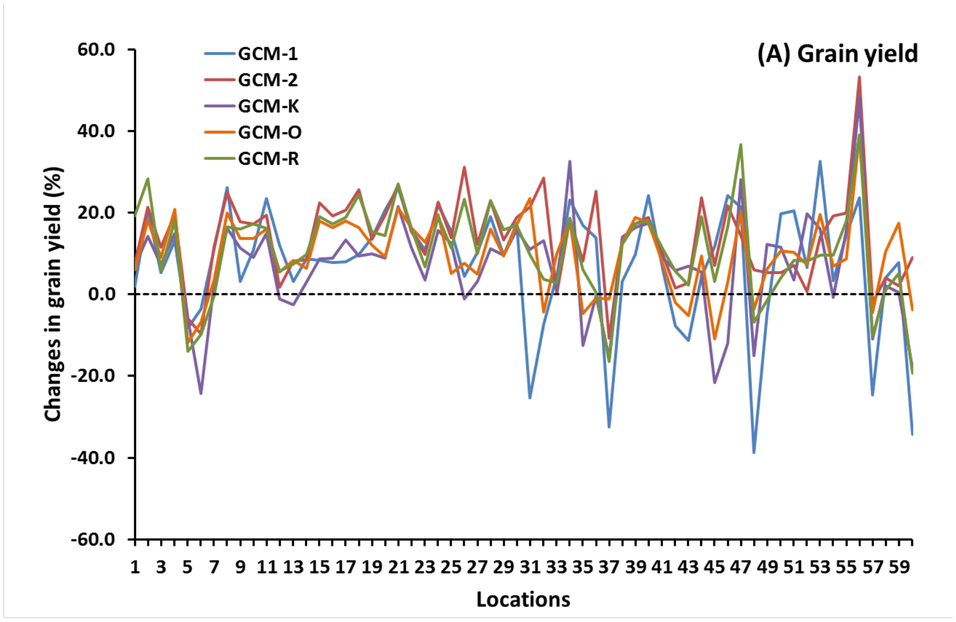

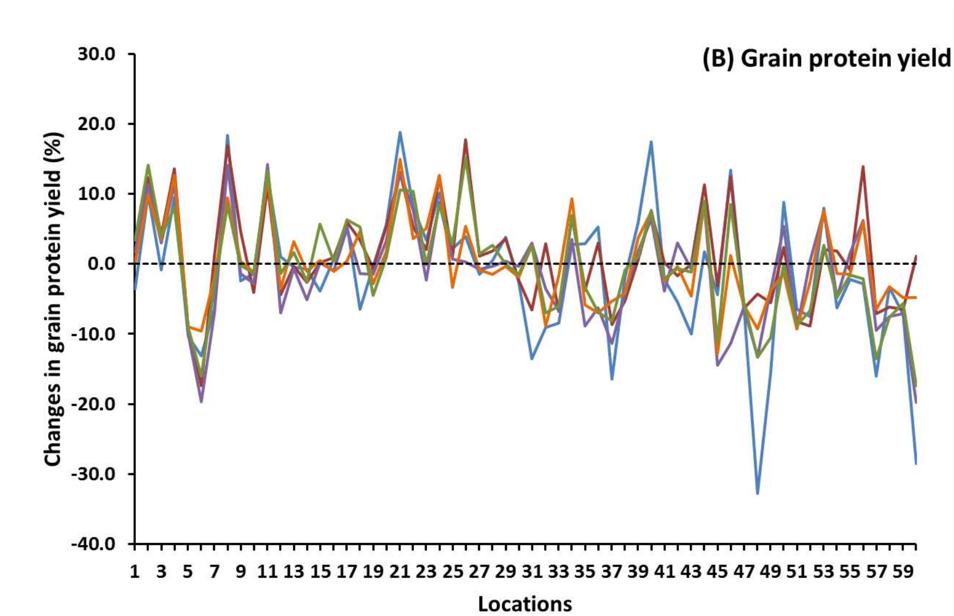

Fig. S23. Simulated wheat grain and protein yield impacts with climate change under five global climate models (GCMs) with genetic adaptation. Relative (**A**) grain yield and (**B**) grain protein yield impact for five GCMs for 2040-2069 (RCP8.5) at the 60 global locations (locations 1 to 30 are irrigated or high rainfall and locations 31 to 60 are rainfed/low input; see Table S5 for details of the locations). Data are ensemble median for 32 crop models (18 for protein), and mean of 30 years using region-specific soils, cultivars, and crop management. Locations are connected by line to improve readability of this figure.

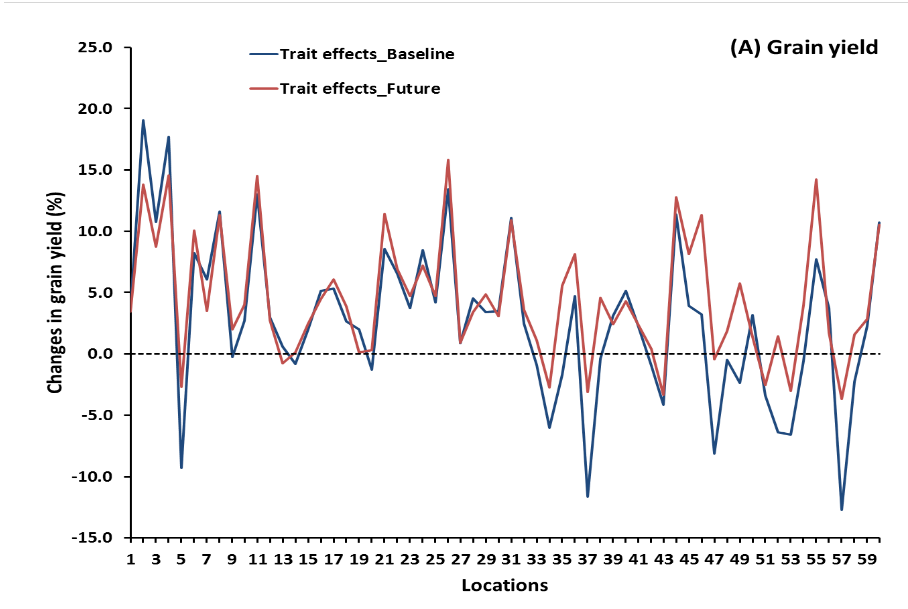

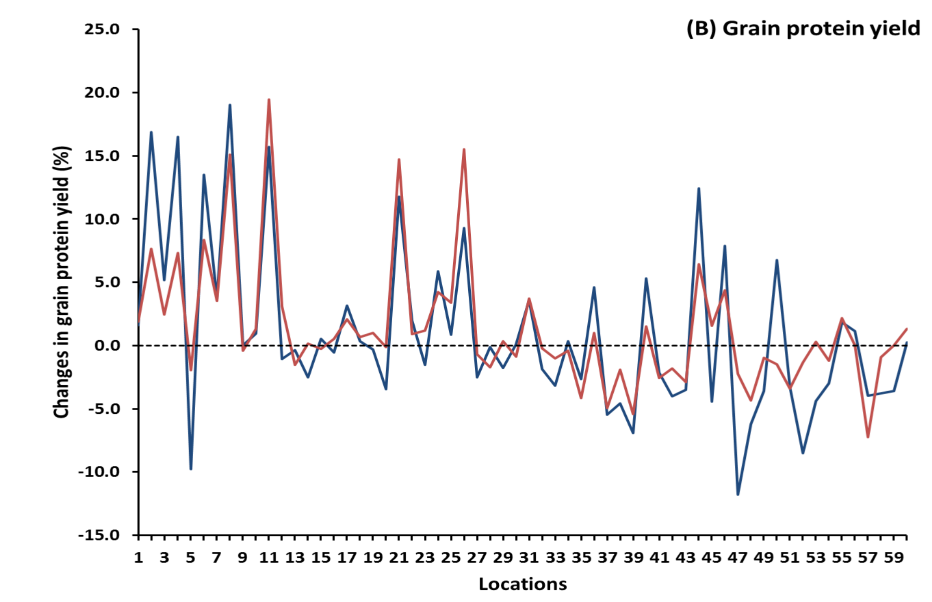

Fig. S24. Simulated effect of genetic adaptation for wheat grain and protein yield under baseline and climate change scenario for 2050s. Relative change in (**A**) grain yield and (**B**) grain protein yield for the baseline (1981-2010) and future climate scenarios for 2040-2069 (RCP8.5, five GCMs) at the 60 global locations (locations 1to 30 are irrigated or high rainfall and locations 31 to 60 are rainfed/low input; see Table S5 for details of the locations). Data are ensemble median for 32 crop models (18 for protein) and mean of 30 years using region-specific soils, cultivars, and crop management. Locations are connected by line to improve readability of this figure.

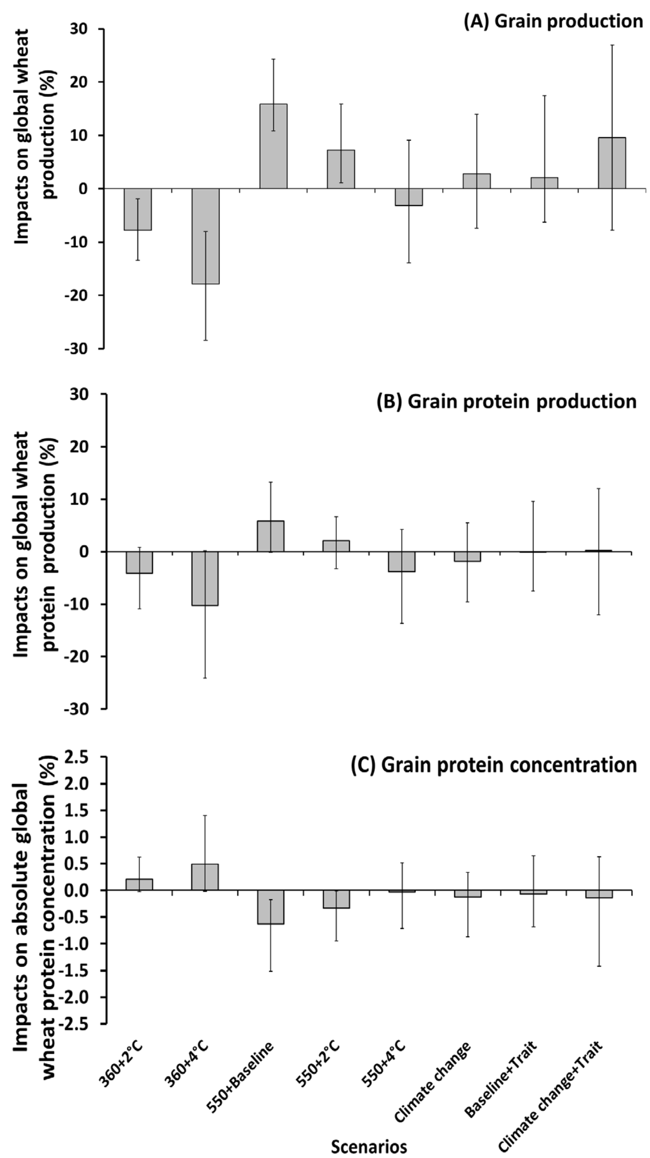

Fig. S25. Simulated global impacts of climate change scenarios on wheat production and protein. Relative impact on (**A**) grain production and (**B**) grain protein production, and (**C**) absolute impact on grain protein concentration for a 2°C (360+2ºC) or 4°C (360+4ºC) temperature increase for the baseline period with historical atmospheric CO_2 concentration (360 ppm) and for a 2°C (550+2ºC) or 4°C (550+4ºC) temperature increase for the baseline period with elevated CO_2 (550 ppm), and climate scenarios for 2040-2069 (RCP8.5, 5 GCMs) without (Climate change) and with (Climate change+Trait) genetic adapation, and for the baseline period with genetic adaptation (Baseline+Trait). Impacts were weighted by production area. Data are ensemble median of 32 crop models (18 for protein) for 360+2ºC, 360+4ºC, 550+Baseline, 550+2ºC, 550+4ºC and Baseline+Trait, and ensemble median across 32 crop models and five GCMs for Climate change and Climate change+Trait, and mean of 30 years using region-specific soils, cultivars, and crop management. Error bars for 360+2ºC, 360+4ºC, 550+Baseline, 550+2ºC, 550+4ºC, and Baseline+Trait are the 25th and 75th percentiles across 32 crop models (18 for grain protein), and for Climate change and Climate change+Trait the 25th and 75th percentiles across 32 crop models and five GCMs together.

References

Aggarwal P, Banerjee B, Daryaei M *et al.* (2006) InfoCrop: A dynamic simulation model for the assessment of crop yields, losses due to pests, and environmental impact of agro-ecosystems in tropical environments. II. Performance of the model. Agricultural Systems, **89**, 47-67.

Al-Mulla Y, Wu J, Singh P, Flury M, Schillinger W, Huggins D, Stockle C (2009) Soil water and temperature in chemical versus reduced-tillage fallow in a Mediterranean climate. Applied Engineering in Agriculture, **25**, 45.

Angulo C, Rötter R, Lock R, Enders A, Fronzek S, Ewert F (2013) Implication of crop model calibration strategies for assessing regional impacts of climate change in Europe. Agricultural and Forest Meteorology, **170**, 32-46.

Araya T, Nyssen J, Govaerts B, Deckers J, Cornelis Wm (2015) Impacts of conservation agriculture-based farming systems on optimizing seasonal rainfall partitioning and productivity on vertisols in the Ethiopian drylands. Soil and Tillage Research, **148**, 1-13.

Asseng S (2004) *Wheat Crop Systems: A Simulation Analysis,* Melbourne, Australia, CSIRO Publishing.

Asseng S, Keating Ba, Fillery Irp *et al.* (1998) Performance of the APSIM-wheat model in Western Australia. Field Crops Research, **57**, 163-179.

Asseng S, Travasso Mi, Ludwig F, Magrin Go (2013) Has climate change opened new opportunities for wheat cropping in Argentina? Climatic change, **117**, 181-196.

Balkovič J, Van Der Velde M, Schmid E *et al.* (2013) Pan-European crop modelling with EPIC: Implementation, up-scaling and regional crop yield validation. Agricultural Systems, **120**, 61-75.

Balkovič J, Van Der Velde M, Skalský R *et al.* (2014) Global wheat production potentials and management flexibility under the representative concentration pathways. Global and Planetary Change, **122**, 107-121.

Bannayan M, Sanjani S, Alizadeh A, Lotfabadi Ss, Mohamadian A (2010) Association between climate indices, aridity index, and rainfed crop yield in northeast of Iran. Field Crops Research, **118**, 105-114.

Basso B, Cammarano D, Troccoli A, Chen D, Ritchie J (2010) Long-term wheat response to nitrogen in a rainfed Mediterranean environment: Field data and simulation analysis. European Journal of Agronomy, **33**, 132-138.

Beringer T, Lucht W, Schaphoff S (2011) Bioenergy production potential of global biomass plantations under environmental and agricultural constraints. Global Change Biology Bioenergy, **3**, 299-312.

Berzsenyi Z, Győrffy B, Lap D (2000) Effect of crop rotation and fertilisation on maize and wheat yields and yield stability in a long-term experiment. European Journal of Agronomy, **13**, 225-244.

Biernath C, Gayler S, Bittner S, Klein C, Hogy P, Fangmeier A, Priesack E (2011) Evaluating the ability of four crop models to predict different environmental impacts on spring wheat grown in open-top chambers. European Journal of Agronomy, **35**, 71-82.

Bondeau A, Smith Pc, Zaehle S, Schaphoff S, Lucht W, Cramer W, Gerten D (2007) Modelling the role of agriculture for the 20th century global terrestrial carbon balance. Global Change Biology, **13**, 679-706.

Boogaard H, Kroes J (1998) Leaching of nitrogen and phosphorus from rural areas to surface waters in the Netherlands. Nutrient Cycling in Agroecosystems, **50**, 321-324.

Brisson N, Gary C, Justes E *et al.* (2003) An overview of the crop model STICS. European Journal of Agronomy, **18**, 309-332.

Brisson N, Mary B, Ripoche D *et al.* (1998) STICS: a generic model for the simulation of crops and their water and nitrogen balances. I. Theory and parameterization applied to wheat and corn. Agronomie, **18**, 311-346.

Cao W, Liu T, Luo W, Wang S, Pan J, Guo W (2002) Simulating organic growth in wheat based on the organ-weight fraction concept. Plant Production Science, **5**, 248-256.
Cao W, Moss Dn (1997) Modelling phasic development in wheat: a conceptual integration of physiological components. Journal of Agricultural Science, **129**, 163-172.
Challinor A, Wheeler T, Craufurd P, Slingo J, Grimes D (2004) Design and optimisation of a large-area process-based model for annual crops. Agricultural and Forest Meteorology, **124**, 99-120.
Chen C, Wang E, Yu Q (2010a) Modeling Wheat and Maize Productivity as Affected by Climate Variation and Irrigation Supply in North China Plain. Agronomy Journal, **102**, 1037-1049.
Chen Y, Carver Bf, Wang S, Cao S, Yan L (2010b) Genetic regulation of developmental phases in winter wheat. Molecular Breeding, **26**, 573-582.
Cuculeanu V, Marica A, Simota C (1999) Climate change impact on agricultural crops and adaptation options in Romania. Climate Research, **12**, 153-160.
Donaldson E, Schillinger Wf, Dofing Sm (2001) Straw production and grain yield relationships in winter wheat. Crop Science, **41**, 100-106.
Fader M, Rost S, Muller C, Bondeau A, Gerten D (2010) Virtual water content of temperate cereals and maize: Present and potential future patterns. Journal of Hydrology, **384**, 218-231.
Fao (1998) World Reference Base for Soil Resources. Rep.84. Rome.
Fao (2010) *Asian wheat producing countries-Uzbekistan-Central Zone*, http://www.fao.org/ag/agp/agpc/doc/field/Wheat/asia/Uzbekistan/agroeco_central.htm (last visited: 09.22.2015).
Ferrise R, Triossi A, Stratonovitch P, Bindi M, Martre P (2010) Sowing date and nitrogen fertilisation effects on dry matter and nitrogen dynamics for durum wheat: An experimental and simulation study. Field Crops Research, **117**, 245-257.
Franzluebbers Aj, Stuedemann Ja (2014) Crop and cattle production responses to tillage and cover crop management in an integrated crop–livestock system in the southeastern USA. European Journal of Agronomy, **57**, 62-70.
Gaiser T, Perkons U, Küpper Pm *et al.* (2013) Modeling biopore effects on root growth and biomass production on soils with pronounced sub-soil clay accumulation. Ecological Modelling, **256**, 6-15.
Gbegbelegbe S, Cammarano D, Asseng S *et al.* (2017) Baseline simulation for global wheat production with CIMMYT mega-environment specific cultivars. Field Crops Research, **202**, 122-135.
Gerten D, Schaphoff S, Haberlandt U, Lucht W, Sitch S (2004) Terrestrial vegetation and water balance - hydrological evaluation of a dynamic global vegetation model. Journal of Hydrology, **286**, 249-270.
Giunta F, Motzo R, Pruneddu G (2007) Trends since 1900 in the yield potential of Italian-bred durum wheat cultivars. European Journal of Agronomy, **27**, 12-24.
Goudriaan J, Van Laar Hh (eds) (1994) *Modelling Potential Crop Growth Processes. Textbook With Exercises,* Dordrecht, The Netherlands, Kluwer Academic Publishers.
Hansen S, Abrahamsen P, Petersen Ct, Styczen M (2012) DAISY: model use, calibration, and validation. Transaction of the ASABE, **55**, 1317-1335.
Hansen S, Jensen H, Nielsen N, Svendsen H (1991) Simulation of nitrogen dynamics and biomass production in winter-wheat using the Danish simulation model DAISY. Fertilizer Research, **27**, 245-259.
He J, Stratonovitch P, Allard V, Semenov Ma, Martre P (2010) Global Sensitivity Analysis of the Process-Based Wheat Simulation Model SiriusQuality1 Identifies Key Genotypic Parameters and Unravels Parameters Interactions. Procedia - Social and Behavioral Sciences, **2**, 7676-7677.
Heng Lk, Asseng S, Mejahed K, Rusan M (2007) Optimizing wheat productivity in two rain-fed environments of the West Asia–North Africa region using a simulation model. European Journal of Agronomy, **26**, 121-129.

Hoogenboom G, White J (2003) Improving physiological assumptions of simulation models by using gene-based approaches. Agronomy Journal, **95**, 82-89.

Hu J, Cao W, Zhang J, Jiang D, Feng J (2004) Quantifying responses of winter wheat physiological processes to soil water stress for use in growth simulation modeling. Pedosphere, **14**, 509-518.

Hu W, Schoenau Jj, Cutforth Hw, Si Bc (2015) Effects of row-spacing and stubble height on soil water content and water use by canola and wheat in the dry prairie region of Canada. Agricultural Water Management, **153**, 77-85.

Huang G, Zhang R, Li G *et al.* (2008) Productivity and sustainability of a spring wheat–field pea rotation in a semi-arid environment under conventional and conservation tillage systems. Field Crops Research, **107**, 43-55.

Hunt La, Pararajasingham S (1995) CROPSIM-wheat - a model describing the growth and development of wheat. Canadian Journal of Plant Science, **75**, 619-632.

Ilbeyi A, Ustun H, Oweis T, Pala M, Benli B (2006) Wheat water productivity and yield in a cool highland environment: Effect of early sowing with supplemental irrigation. Agricultural Water Management, **82**, 399-410.

Iqbal M, Akhter J, Mohammad W, Shah S, Nawaz H, Mahmood K (2005) Effect of tillage and fertilizer levels on wheat yield, nitrogen uptake and their correlation with carbon isotope discrimination under rainfed conditions in north-west Pakistan. Soil and Tillage Research, **80**, 47-57.

Islam T (1991) Water use of a winter wheat cultivar (Triticum aestivum). Agricultural Water Management, **19**, 77-84.

Izaurralde R, Solberg E, Nyborg M, Malhi S (1998) Immediate effects of topsoil removal on crop productivity loss and its restoration with commercial fertilizers. Soil and Tillage Research, **46**, 251-259.

Izaurralde R, Williams Jr, Mcgill Wb, Rosenberg Nj, Jakas Mq (2006) Simulating soil C dynamics with EPIC: Model description and testing against long-term data. Ecological Modelling, **192**, 362-384.

Izaurralde Rc, Mcgill Wb, Williams Jr (2012) Development and application of the EPIC model for carbon cycle, greenhouse-gas mitigation, and biofuel studies. In: *Managing agricultural greenhouse gases: Coordinated agricultural research through GRACEnet to address our changing climate.* (eds Liebig Ma, Franzluebbers Aj, Follett Rf) pp Page. Amsterdam, Elsevier.

Jamieson P, Semenov M (2000) Modelling nitrogen uptake and redistribution in wheat. Field Crops Research, **68**, 21-29.

Jamieson P, Semenov M, Brooking I, Francis G (1998) Sirius: a mechanistic model of wheat response to environmental variation. European Journal of Agronomy, **8**, 161-179.

Jones J, Hoogenboom G, Porter C *et al.* (2003) The DSSAT cropping system model. European Journal of Agronomy, **18**, 235-265.

Kassie Bt, Asseng A, Porter Ch, Royce F (2016) Performance of DSSAT-Nwheat across a wide range of current and future growing conditions. Field Crops Research, **81**, 27-36.

Keating Ba, Carberry Ps, Hammer Gl *et al.* (2003) An overview of APSIM, a model designed for farming systems simulation. European Journal of Agronomy, **18**, 267-288.

Kersebaum K (2007) Modelling nitrogen dynamics in soil-crop systems with HERMES. Nutrient Cycling in Agroecosystems, **77**, 39-52.

Kersebaum Kc (2011) Special features of the HERMES model and additional procedures for parameterization, calibration, validation, and applications. Ahuja, L.R. and Ma, L. (eds.). Methods of introducing system models into agricultural research. Advances in Agricultural Systems Modeling Series 2, Madison (ASA-CSSA-SSSA), 65-94.

Khalil F, Samiha O, Nemat Allah O, Ghamis A (2011) DETERMINATION OF AGRO-CLIMATIC ZONES IN EGYPT USING A ROBUST STATISTICAL PROCEDURE. Fifteenth International Water Technology Conference, **IWTC** - **15**.

Kiniry Jr, Williams J, Major D *et al.* (1995) EPIC model parameters for cereal, oilseed, and forage crops in the northern Great Plains region. Canadian Journal of Plant Science, **75**, 679-688.
Latiri K, Lhomme J-P, Annabi M, Setter Tl (2010) Wheat production in Tunisia: progress, inter-annual variability and relation to rainfall. European Journal of Agronomy, **33**, 33-42.
Latta J, O'leary G (2003) Long-term comparison of rotation and fallow tillage systems of wheat in Australia. Field Crops Research, **83**, 173-190.
Lawless C, Semenov M, Jamieson P (2005) A wheat canopy model linking leaf area and phenology. European Journal of Agronomy, **22**, 19-32.
Li C, Cao W, Zhang Y (2002) Comprehensive Pattern of Primordium Initiation in Shoot Apex of Wheat. ACTA Botanica Sinica, 273-278.
Li S, Wheeler T, Challinor A, Lin E, Xu Y, Ju H (2010) Simulating the Impacts of Global Warming on Wheat in China Using a Large Area Crop Model. Acta Meteorologica Sinica, **24**, 123-135.
Lithourgidis A, Damalas C, Gagianas A (2006) Long-term yield patterns for continuous winter wheat cropping in northern Greece. European Journal of Agronomy, **25**, 208-214.
Maiorano A, Martre P, Asseng S *et al.* (2017) Crop model improvement reduces the uncertainty of the response to temperature of multi-model ensembles. Field Crops Research, **202**, 5-20.
Malr (2003) Bulletin of Agriculture Economics, Central Administration of Agriculture Economics, Ministry of Agriculture and Land Reclamation. Dokki, Egypt.
Martre P, Jamieson Pd, Semenov Ma, Zyskowski Rf, Porter Jr, Triboi E (2006) Modelling protein content and composition in relation to crop nitrogen dynamics for wheat. European Journal of Agronomy, **25**, 138-154.
Mossé J, Huet J, Baudet J (1985) The amino acid composition of wheat grain as a function of nitrogen content. Journal of Cereal Science, **3**, 115-130.
Müller C, Eickhout B, Zaehle S, Bondeau A, Cramer W, Lucht W (2007) Effects of changes in CO2, climate, and land use on the carbon balance of the land biosphere during the 21st century. Journal of Geophysical Research-Biogeosciences, **112**.
Nash Je, Sutcliffe Jv (1970) River flow forecasting through conceptual models part I - A discussion of principles. Journal of Hydrology, **10**, 282-290.
Nendel C, Berg M, Kersebaum K *et al.* (2011) The MONICA model: Testing predictability for crop growth, soil moisture and nitrogen dynamics. Ecological Modelling, **222**, 1614-1625.
O'leary Gj, Christy B, Nuttall J *et al.* (2015) Response of wheat growth, grain yield and water use to elevated CO under a Free-Air CO Enrichment (FACE) experiment and modelling in a semi-arid environment. Global Change Biology, **21**, 2670-2686.
Oleary G, Connor D (1996a) A simulation model of the wheat crop in response to water and nitrogen supply .1. Model construction. Agricultural Systems, **52**, 1-29.
Oleary G, Connor D (1996b) A simulation model of the wheat crop in response to water and nitrogen supply .2. Model validation. Agricultural Systems, **52**, 31-55.
Oleary G, Connor D, White D (1985) A simulation-model of the development, growth and yield of the wheat crop. Agricultural Systems, **17**, 1-26.
Pan J, Zhu Y, Cao W (2007) Modeling plant carbon flow and grain starch accumulation in wheat. Field Crops Research, **101**, 276-284.
Pan J, Zhu Y, Jiang D, Dai Tb, Li Yx, Cao Wx (2006) Modeling plant nitrogen uptake and grain nitrogen accumulation in wheat. Field Crops Research, **97**, 322-336.
Pavlova Vn, Varcheva Se, Bokusheva R, Calanca P (2014) Modelling the effects of climate variability on spring wheat productivity in the steppe zone of Russia and Kazakhstan. Ecological Modelling, **277**, 57-67.
Pecetti L, Hollington P (1997) Application of the CERES-Wheat simulation model to durum wheat in two diverse Mediterranean environments. European Journal of Agronomy, **6**, 125-139.

Porter J (1984) A model of canopy development in winter wheat. The Journal of Agricultural Science, **102**, 383-392.

Porter Jr (1993) AFRCWHEAT2: a model of the growth and development of wheat incorporating responses to water and nitrogen. European Journal of Agronomy, **2**, 69-82.

Portmann Ft, Siebert S, Döll P (2010) MIRCA2000–Global monthly irrigated and rainfed crop areas around the year 2000: A new high‐resolution data set for agricultural and hydrological modeling. Global biogeochemical cycles, **24**.

Priesack E, Gayler S, Hartmann H (2006) The impact of crop growth sub-model choice on simulated water and nitrogen balances. Nutrient Cycling in Agroecosystems, **75**, 1-13.

Ramirez-Rodrigues Ma, Asseng S, Fraisse C, Stefanova L, Eisenkolbi A (2014) Tailoring wheat management to ENSO phases for increased wheat production in Paraguay. Climate Risk Management, **3**, 24-38.

Reynolds Mp, Balota M, Delgado Mib, Amani I, Fischer Ra (1994) Physiological and morphological traits associated with spring wheat yield under hot, irrigated conditions. Australian Journal of Plant Physiology, **21**, 717-730.

Ritchie Jt, Godwin Dc, Otter-Nacke S (1985) *CERES-wheat: A user-oriented wheat yield model. Preliminary documentation*.

Ritchie S, Nguyen H, Holaday A (1987) Genetic diversity in photosynthesis and water-use efficiency of wheat and wheat relatives. Journal of Cellular Biochemistry, 43-43.

Romero Cc, Hoogenboom G, Baigorria Ga, Koo J, Gijsman Aj, Wood S (2012) Reanalysis of a global soil database for crop and environmental modeling. Environmental Modelling & Software, **35**, 163-170.

Rost S, Gerten D, Bondeau A, Lucht W, Rohwer J, Schaphoff S (2008) Agricultural green and blue water consumption and its influence on the global water system. Water Resources Research, **44**.

Royo C, Villegas D, Rharrabti Y, Blanco R, Martos V, García Del Moral L (2006) Grain growth and yield formation of durum wheat grown at contrasting latitudes and water regimes in a Mediterranean environment. Cereal Research Communications, **34**, 1021-1028.

Rötter Rp, Palosuo T, Kersebaum Kc *et al.* (2012) Simulation of spring barley yield in different climatic zones of Northern and Central Europe: a comparison of nine crop models. Field Crops Research, **133**, 23-36.

Schillinger Wf, Schofstoll Se, Alldredge Jr (2008) Available water and wheat grain yield relations in a Mediterranean climate. Field Crops Research, **109**, 45-49.

Semenov M, Shewry P (2011) Modelling predicts that heat stress, not drought, will increase vulnerability of wheat in Europe. Scientific Reports, **1**.

Senthilkumar S, Basso B, Kravchenko An, Robertson Gp (2009) Contemporary Evidence of Soil Carbon Loss in the US Corn Belt. Soil Science Society of America Journal, **73**, 2078-2086.

Shibu M, Leffelaar P, Van Keulen H, Aggarwal P (2010) LINTUL3, a simulation model for nitrogen-limited situations: Application to rice. European Journal of Agronomy, **32**, 255-271.

Singels A, De Jager J (1991) Determination of optimum wheat cultivar characteristics using a growth model. Agricultural Systems, **37**, 25-38.

Soltani A, Maddah V, Sinclair T (2013) SSM-Wheat: a simulation model for wheat development, growth and yield. International Journal of Plant Production, **7**, 711-740.

Sommer R, Piggin C, Haddad A, Hajdibo A, Hayek P, Khalil Y (2012) Simulating the effects of zero tillage and crop residue retention on water relations and yield of wheat under rainfed semiarid Mediterranean conditions. Field Crops Research, **132**, 40-52.

Spitters Cjt, Schapendonk Ahcm (1990) Evaluation of breeding strategies for drought tolerance in potato by means of crop growth simulation. Plant and Soil, **123**, 193-203.

Steduto P, Hsiao T, Raes D, Fereres E (2009) AquaCrop-The FAO Crop Model to Simulate Yield Response to Water: I. Concepts and Underlying Principles. Agronomy Journal, **101**, 426-437.

Steduto P, Pocuca V, Caliandro A, Debaeke P (1995) An evaluation of the crop-growth simulation submodel of epic for wheat grown in a Mediterranean climate with variable soil-water regimes. European Journal of Agronomy, **4**, 335-345.

Stenger R, Priesack E, Barkle G, Sperr C (1999) Expert-N A tool for simulating nitrogen and carbon dynamics in the soil-plant-atmoshpere system. pp Page, New Zealand, Land Treatment collective proceedings Technical Session.

Stockle C, Donatelli M, Nelson R (2003) CropSyst, a cropping systems simulation model. European Journal of Agronomy, **18**, 289-307.

Taha Mh (2000) Soil fertility management in Egypt. Regional Workshop on Soil Fertility Management Through Farmer Field Schools in the Near East,Amman, Jordan,, 2–5.

Tao F, Yokozawa M, Zhang Z (2009a) Modelling the impacts of weather and climate variability on crop productivity over a large area: A new process-based model development, optimization, and uncertainties analysis. Agricultural and Forest Meteorology, **149**, 831-850.

Tao F, Zhang Z (2010) Adaptation of maize production to climate change in North China Plain: Quantify the relative contributions of adaptation options. European Journal of Agronomy, **33**, 103-116.

Tao F, Zhang Z (2013) Climate change, wheat productivity and water use in the North China Plain: A new super-ensemble-based probabilistic projection. Agricultural and Forest Meteorology, **170**, 146-165.

Tao F, Zhang Z, Liu J, Yokozawa M (2009b) Modelling the impacts of weather and climate variability on crop productivity over a large area: A new super-ensemble-based probabilistic projection. Agricultural and Forest Meteorology, **149**, 1266-1278.

Tavakkoli Ar, Oweis Ty (2004) The role of supplemental irrigation and nitrogen in producing bread wheat in the highlands of Iran. Agricultural Water Management, **65**, 225-236.

Triboï E, Triboï-Blondel A, Martignac M, Falcimagne R (1996) Experimental device for studying post-anthesis canopy functioning in relation to grain quality. In: *Proc 4th European Society of Agronomy Congress, Amsterdam Academic Press, Wageningen, The Netherlands, pp68-69.* pp Page.

Van Rees H, Mcclelland T, Hochman Z, Carberry P, Hunt J, Huth N, Holzworth D (2014) Leading farmers in South East Australia have closed the exploitable wheat yield gap: Prospects for further improvement. Field Crops Research, **164**, 1-11.

Wang E, Engel T (2000) SPASS: a generic process-oriented crop model with versatile windows interfaces. Environmental Modelling & Software, **15**, 179-188.

Wang E, Robertson Mj, Hammer Gl *et al.* (2002) Development of a generic crop model template in the cropping system model APSIM. European Journal of Agronomy, **18**, 121-140.

Webber H, Gaiser T, Oomen R *et al.* (2016) Uncertainty in future irrigation water demand and risk of crop failure for maize in Europe. Environmental Research Letters, **11**, 074007.

Weir A, Bragg P, Porter J, Rayner J (1984) A winter wheat crop simulation model without water or nutrient limitations. The Journal of Agricultural Science, **102**, 371-382.

Williams J (1995) *The EPIC model in: Computer Models of Watershed Hydrology*, Water Resources Publications, Highlands Ranch, Colorado, USA.

Williams Jr, Jones Ca, Kiniry Jr, Spanel Da (1989) The EPIC crop growth model. Transactions of the ASAE, **32**, 497-511.

Yan M, Cao W, C. Li Zw (2001) Validation and evaluation of a mechanistic model of phasic and phenological development in wheat. Chinese Agricultural Science, **1**, 77-82.

Yin X, Van Laar Hh (2005) *Crop systems dynamics: an ecophysiological simulation model of genotype-by-environment interactions,* Wageningen, The Netherlands, Wageningen Academic Publishers.

1